26th Annual AHS Student Design Competition

2009 Request for Proposal (RFP)

For

Non-conventional rotor drive

Sponsored by

and

Proposal for 26th AHS Student Design Competition

by

NUAA Undergraduate Student Design Team

College of Aerospace Engineering

Nanjing University of Aeronautics and Astronautics, China

May 31, 2009

NUAA Undergraduate Student Design Team

Fei Qin(秦飞)	Undergraduate student	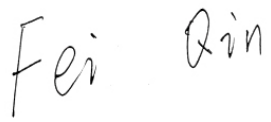
Xiao Chen(陈晓)	Undergraduate student	
Shuai He(何帅)	Undergraduate student	
Xinquan Zhou(周新权)	Undergraduate student	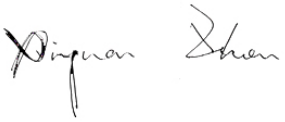
Siyuan Yang(杨思远)	Undergraduate student	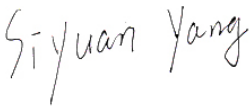
Yixin Han(韩意新)	Undergraduate student	
Dr. Pinqi Xia(夏品奇)	Faculty advisor	

Contents

List of Figures

List of Tables

Symbols

a_{1s}	Longitudinal Flap Angle
b_{1s}	Lateral Flap Angle
b	Main Blade Chord Length
C_T	Lift Coefficient
C_{y7}	Blade Lift Coefficient
C_{x7}	Blade Drag Coefficient
$\widetilde{C}_x$	Section Parasite Coefficient
C_e	Fuel Consumption
G	Gross Weight
G_u	Payload
$\overline{G}_f$	Relative Fuel Weight
$\overline{G}$	Weight Efficiency
J	Empirical Factor of Induced Power
k	Number of Blades
K_T	Lift Modifying Coefficient
m_k	Required Power Coefficient
m_{ki}	Induced Power Coefficient
m_{kx}	Profile Power Coefficient
m_{kf}	Parasite Power Coefficient
M	Mach Number
M_k	Rotor Torque
N_r	Required Power

N_e	Efficient Power
N_t	Takeoff Power
p	Disk Load
p_b	Blade Loading
R	Disk Radius
V_y	Rate of Ascent
$\bar{v}_1$	Induced Velocity
$\overline{V_0}$	Forward Flight Velocity
α	Angle of Attack
α_f	Body Pitch Attitude
β	Sideslip Angle
Ω	Rotor Rotational Speed
ΩR	Blade Tip Speed
σ	Rotor Disk Solidity
λ_0	Rotor Inflow Ratio
μ	Rotor Advance Ratio
$\sum C_x S$	Body Parasite Area
ρ	Air Density
γ_b	Blade Lock Number
δ	Rotor Shaft Rake Angle
θ_2	Longitudinal Cyclic Pitch Angle
φ	Collective Pitch
ψ	Azimuth Angle

Executive Summary

This proposal is submitted to the AHS International for the 26^{th} Annual AHS Student Design Competition by the undergraduate design team in the College of Aerospace Engineering, Nanjing University of Aeronautics and Astronautics. The designed rotorcraft is a new kind of advanced VTOL concept helicopter, containing a stopped rotor, blade tip rocket jet and vectored thrust ducted propeller, and with no tail rotor and no gearbox. During the design process, every student of the team gained enormous knowledge and experience, as well as enhancing our ability to cooperate as a team. The new helicopter was designed to reach the objectives of improvements on range, speed, and payload under the operational conditions. As a completely new type of helicopter, it has its originality and a detailed design and analysis including the concept design, aerodynamics design, flight performance analysis, rotor design, blade tip rocket jet design, vectored thrust ducted propeller design, fuselage design, and landing system design. Because blade tip rocket jet is used, there is no need to use the traditional anti-torque system. Profiting from the new rotor drive system, the weight of helicopter is reduced to improve the weight efficiency and vibration reduction. Flight direction of the helicopter is controlled by the vectored thrust ducted propeller. By using vectored thrust ducted propeller, the flight speed is increased a lot. The flank wings are also used to low the rotor load in forward flight. Particularly in maneuver, the wings will increase the largest flight overload of helicopter. Furthermore, the streamlined fuselage and retractile undercarriage are adopted to reduce the body drag.

The main parameters of the new helicopter were determined as MTOW=4000kg, weight efficiency $\overline{G}$ =0.536, rotor diameter D=12m, disk load p=346.8 N/m^2, number of blades k=4, blade tip speed ΩR=220m/s, rotor rotational speed Ω=350rpm, solidity σ=0.19. The flight performance were calculated as the maximum speed 396km/h, cruise speed 350km/h, maximum range 1417.5km, hover ceiling with ground effect 3429km, and 2936km with no ground effect. Comparing with the performance of the reference helicopter SA365N, the weight efficiency 0.495, maximum speed 306km/h, cruise speed 260km/h, maximum range 882km, hover ceiling with ground effect 2050km, and 1050km with no ground effect, the new designed helicopter has a greater improvement on range, speed and payload, and has the advantage of compact structure, low noise and vibration reduction. The new helicopter can address many kings of missions such as reconnaissance, paramilitary, utility transport, VIP transport, fire fighting, succor and so on at a high cruise speed and long range. The blade tip rocket jet drive system is an ideal conception for the future helicopter.

Chapter 1 Introduction

1.1 Mission Description and Design Objectives

The RFP for the 26 Annual AHS Student Design Competition sponsored by the American Helicopter Society and Agusta Westland specifies that a non-conventional change to the rotor/drive system of a helicopter is to be designed for an existing and in-service airframe which has a maximum takeoff weight between 3500 and 5500 Kg. It is also clearly stated that all new concepts are to be imaginative yet remain practical. Students must evaluate technology readiness levels for the various technologies to be employed in their design as well as justify the trade-offs of such technologies. By using state-of-the-art technologies, a new rotor/drive system has been designed including attention to all necessary subsystems.

Very few rotor/drive designs are currently in service with the acceptance of the industry. Students are not to merely switch from one such in service design to another but rather design an entirely new system by which to achieve the particular traits that are exhibited by a helicopter.
These traits are not to be ignored with a redesign of the rotor/drive system either as the helicopter must maintain hover and VTOL capabilities. Additionally, the designs employed by students must show an increase in range, speed performance of the rotorcraft.

The student team has worked to construct a design which fulfills and exceeds all requirements set forth in the RFP. The team decided to focus improvements on range and speed, and performance of range, speed and load has seen an increase with a change in rotor/drive systems as defined herein.
The new rotorcraft has excellent performance with its range 1417.5km, the maximum hover ceiling 2936m and the maximum forward speed 396km/h. Through its innovative design, the rotorcraft is greatly advanced in its speed, range and vibration, comparing with the reference helicopters, SA365N.

1.2 Design Features

Many innovative concept designs were incorporated in the rotorcraft design to improve its performance on the range, speed and load.

(1) A blade tip rocket jet drive system, which can get rid of gearbox and anti-torque system, the configuration is simplified, so more load can be taken, comparing with the traditional tail rotor system.

(2) Flank wings, which can low the rotor loading in high flight speed.

(3) A stopped rotor, which can reduce the noise and increase the speed.

(4) A streamlined fuselage and retractile undercarriage, which can reduce parasite power.

(5) A vectored thrust ducted propeller produce the forces to supply the yaw and pitching moments for the rotorcraft and control the flight directions.

The 3D view of the new helicopter is shown in Figure 1.1. The detailed design of the new rotorcraft has been described in the chapters. In Chapter 2, the main parameters of the helicopter including gross weight, disk load, blade tip speed, solidity, number of blades and engine power are determined. The concept design ideas of the helicopter are described and the designed configuration is plotted in Chapter 3. The rotor system design including the choice of the rotor aerodynamics shape, structural design of rotor blades, the design of bearingless rotor is given in Chapter 4. In Chapter 5, rotor propulsion system design including engine selection, determination of solid rocket engine parameters, engine component design, the specific analysis. Vectored thrust ducted propeller system Design is given in Chapter 6, including power system selection, aerodynamic characteristics analysis, propeller design, the ducted body design. The structure design including airframe structure design, overload landing analysis, the landing gear design, bulkhead design, is given in Chapter 7. The flight performances including required power, vertical flight performance, climb performance, range, flight time, maximum forward flight speed and minimum rotational sliding speed are described in Chapter 8.

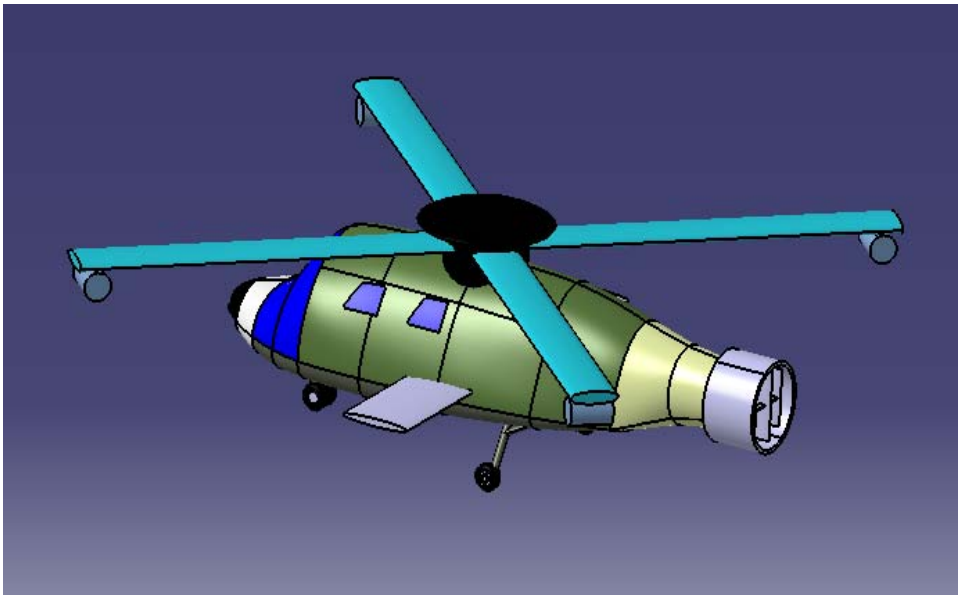

Figure 1.1 3D View of the New Helicopter

Chapter 2 Determination of Main Parameters

2.1 Estimation of Gross Weight

The gross weight of the new helicopter was estimated by the statistic data of other similar helicopters, mainly determined by SA365N. The empty weight of SA365N is 1945kg, the maximum take-off weight (MTOW) is 3850kg. So the weight efficiency is 0.495, determined by the formula $\overline{G} = (G - G_{em})/G$. The rotorcraft's empty weight is provisionally estimated as 1854.6kg, the MTOW is 4000kg and the weight efficiency is 0.536. Compared with SA365N, the weight efficiency is increased a little.

2.2 Estimation of Disk Load

The requirement for estimating disk load is to ensure that G_u has the largest property in gross weight under the certain condition of performance. Disk load is determined by referring to the similar helicopter SA365N. The diameter of disk should be corresponding to the blade tip speed. Then disk load was determined as $p = G/(\pi R^2) = 346.8N/m^2$

2.3 Number of Blades

The advantages of large k are to reduce the vibration of the blade and the helicopter, as well as improve the performance during flight. On the other hand, the disadvantages of large number k are to make the rotor hub more complicated, to increase the parasite power and the maintenance of the rotor. Small number k means a simple rotor hub, light body, low cost and the little disturbance of blade tip vortex.

According to the empirical formula $C_L \times 2k = (C_T/\sigma) \times 2k$, its result should be around 0.42. Referring to SA365N, 4 blades were selected, which means k=4, $C_T \approx 11.7 \times 10^{-3}$, then $C_L \times 2k \approx 0.49$, which is in a normal range.

2.4 Blade Tip Speed and Solidity

When determining blade speed ΩR, some points should be considered: (1) the rotor must store enough kinetic energy to achieve the auto rotational landing; (2) the stalling speed of the blade tip; (3) the acoustic boundary. Referring to the empirical calculation, BTS was estimated as $\Omega R = V_{\max}/\mu_{\max} = V_{\max}/0.3$. Considering that the helicopter's rotor will stop rotating when the speed achieves 280km/h (According to calculation, it'll take 104 seconds to reach this speed.), so the helicopter flight mode is under 240km/h. $V_{\max}$ is estimated as 240km/h., and ΩR is 220 m/s. After estimating BTS, blade chord is estimated as b=0.9m by considering the air-flow separation and enough lift to carry the helicopter. Then the solidity is calculated as $\sigma = kb/\pi R = 0.19$, and

blade loading is calculated as $p_b = p/\sigma = 1825N/m^2$. The radius of the disk was determined as R=6m, then the rotor rotational speed is determined as $\Omega = 350rpm$.

2.5 Estimation of Engine Power

(1) Blade Tip Rocket Jet Power

When considering hover, every part of the rotor power was calculated, including m_{kx} and m_{ki}, then the required rotor power was $N_r = 737kw$. According to the statistic data, power transfer coefficient of each part is

$$\left.\begin{array}{l}\varsigma_{drive} = 0.94 \sim 0.96 \\ \varsigma_{\text{radiate}} = 0.95 \sim 0.97 \\ \varsigma_{tail} = 0.92 \sim 0.95 \\ \varsigma_{others} = 0.99\end{array}\right\} \quad \varsigma = 0.80 \sim 0.88$$

For blade tip rocket jet is used, there is no loss of drive and tail, estimating ς as 0.94, so the efficient power of the rocket jet should be $N_e = N_r/\varsigma = 784kw$, and the take off power is $N_t = N_e/(90\%) = 784kw/(90\%) = 871kw$.

(2) Turbopropeller Power

Following the process as below, the turbopropeller power was calculated. (a) Flank wings' lift $L_1 = a_{\infty 1}\alpha_1 \frac{1}{2}\rho V^2 b_1 l$; (b) Flank wings' drag $D_1 = C_{x1}\frac{1}{2}\rho V^2 b_1 l$; (c) Rotor's lift $L_2 = G - L_1$; (d) Blade's angle of attack $\alpha_2 = L_2/[\frac{1}{2}\rho(\frac{\sqrt{2}}{2}V)^2 bR]$; (e) Rotor's drag is D_2 which should be calculated in different conditions. $D_2 = 0$ if the speed is less than 280km/h, otherwise, $D_2 = C_x\frac{1}{2}\rho(\frac{\sqrt{2}}{2}V)^2\frac{\sqrt{2}}{2}bR$; (f) Airframe's drag $D_3 = (\sum C_x S)\frac{1}{2}\rho V^2$; (g) The total drag of the rotorcraft $D = D_1 + D_2 + D_3$; (h) Turbopropeller's required power $N = DV$. Finally, the turbopropeller's cruise power is 1009kw, and maximum required power is 1431kw.

Chapter 3 Configuration Design

3.1 Collocation of Rotor

Because the rotorcraft flies in two flight modes, helicopter flight mode and airplane flight mode, the anteversion angle of the rotor shaft is zero.

3.2 Arrangement and Main Parameter of Flank Wings

The flank wings will low the rotor load in forward flight. Particularly in maneuver, the wings will increase the largest helicopter flight overload. However, in hover and vertical climb, the flank wings will produce a downward aerodynamic resistance, and increase the helicopter weight. In forward flight, the flank wings' induced resistance will also increase the required power. In autorotation flight, because the flank wings' angle of attack increases, lift increases, resulting in decreased tension of rotor, which brings a negative effect on the autorotation characteristics. So the choice of wing's type, size, aspect ratio, flat shape, angle and other parameters should be considered synthetically to minimize adverse effects to meet the dynamic, aerodynamic performance and flight qualities requirements.

The flank wings should be arranged in reward of the whole helicopter's barycenter, so the wings could play the role of stability to increase the static longitudinal stability of the entire helicopter. Some typical helicopter Statistics are listed in Table 3.1. The curve about typical helicopter rotor diameter and flank wingspan is shown in Figure 3.1.

Table 3.1 Some Typical Helicopter Rotor Diameter and Flank Wingspan Statistics

Type of helicopter	rotor diameter/m	flank wings wingspan/m
EC665	13	4.52
AH-64	14.63	5.23
S-72X1	17.59	13.75
Bell-209	14.63	3.28
Bell-409	15.54	5.24
CSH-2	15.58	6.34
Ka-50	14.5	7.34
Mi-6	35.00	15.30
Mi-24	17.30	6.66
OH-1	11.5	3
A129	11.9	3.20

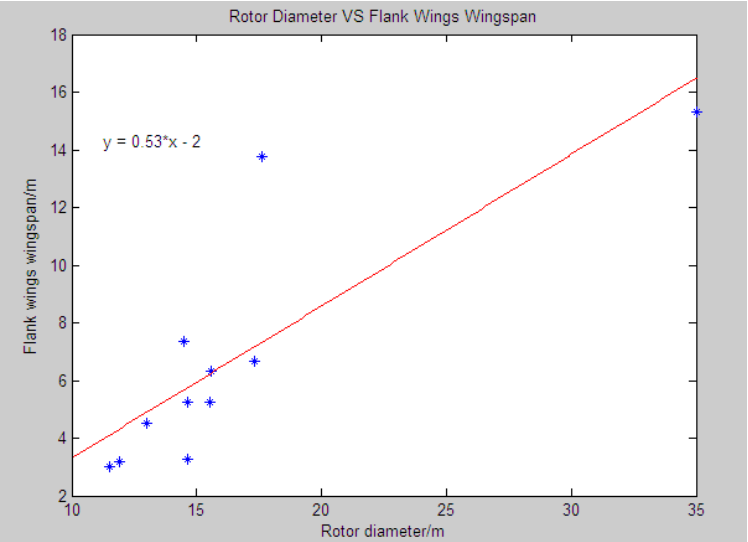

Figure 3.1 Rotor Diameter VS Flank Wingspan

The diameter of the new helicopter is 12m, according to the above curve, flank wings wingspan is estimated as 4m. Taking into account good lift characteristics of flank wings, OA213 airfoil is selected, and chord length is 1.25m.

3.3 Layout of Turbopropeller

Considering the weight of turbopropeller, it should be located as close as possible to the rotor shaft. Otherwise, it is adverse for barycenter balancing. Finally, the distance between turbopropeller and rotor axis was determined as 2.2m.

According to the above analysis, the configuration of the helicopter was determined initially. The multi-directional view of the helicopter is shown in Figure 3.2.

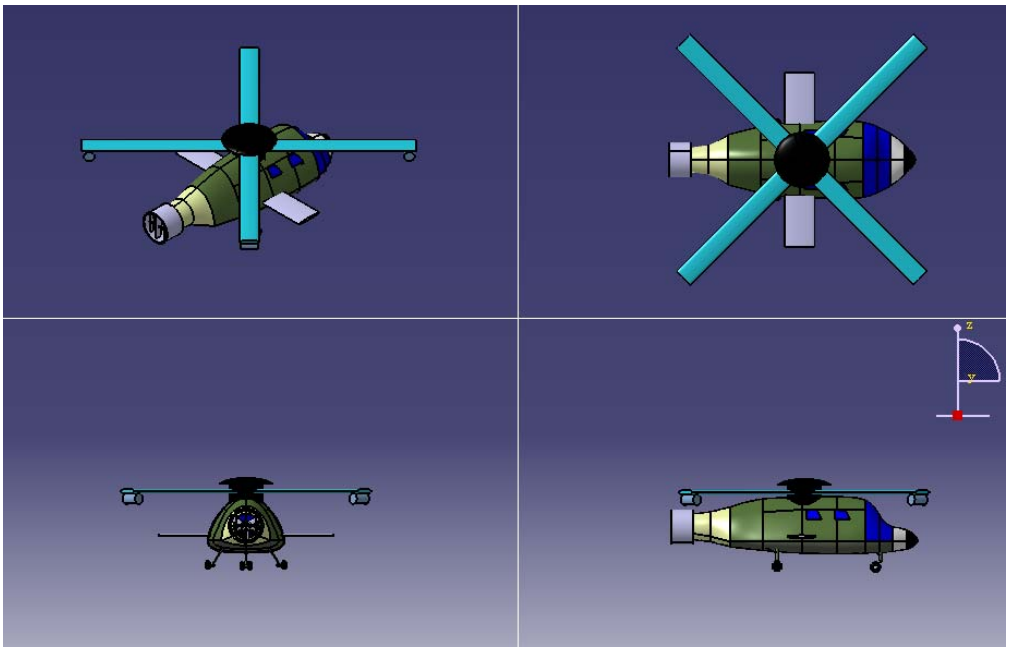

Figure 3.2 Multi-directional View of the New Helicopter

3.4 General Arrangement

General arrangement mainly determines the overall layout of components and equipment. The final size chart is Figure 3.3 and arrangement for helicopter is shown in Figure 3.4.

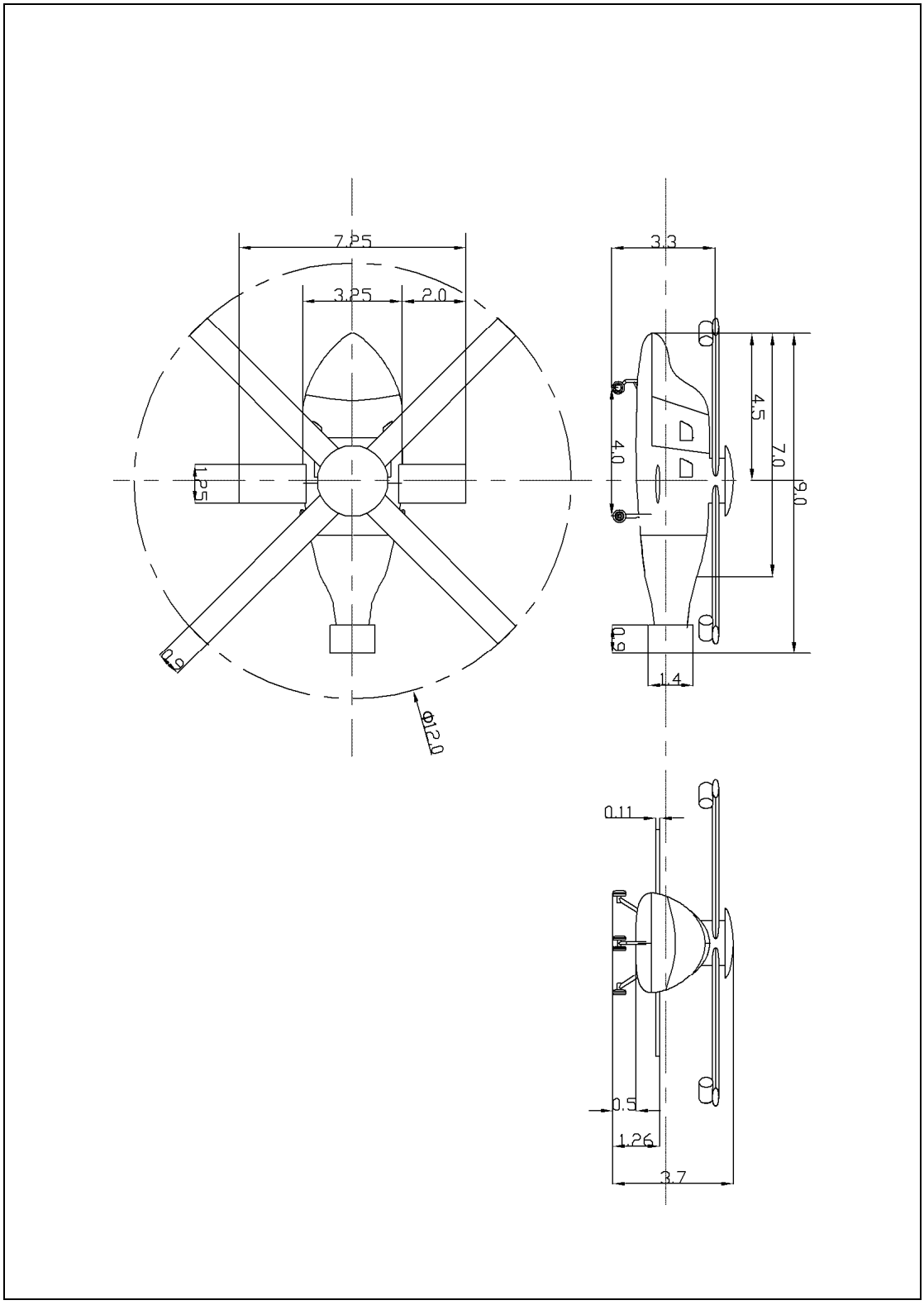

Figure 3.3 Size Chart

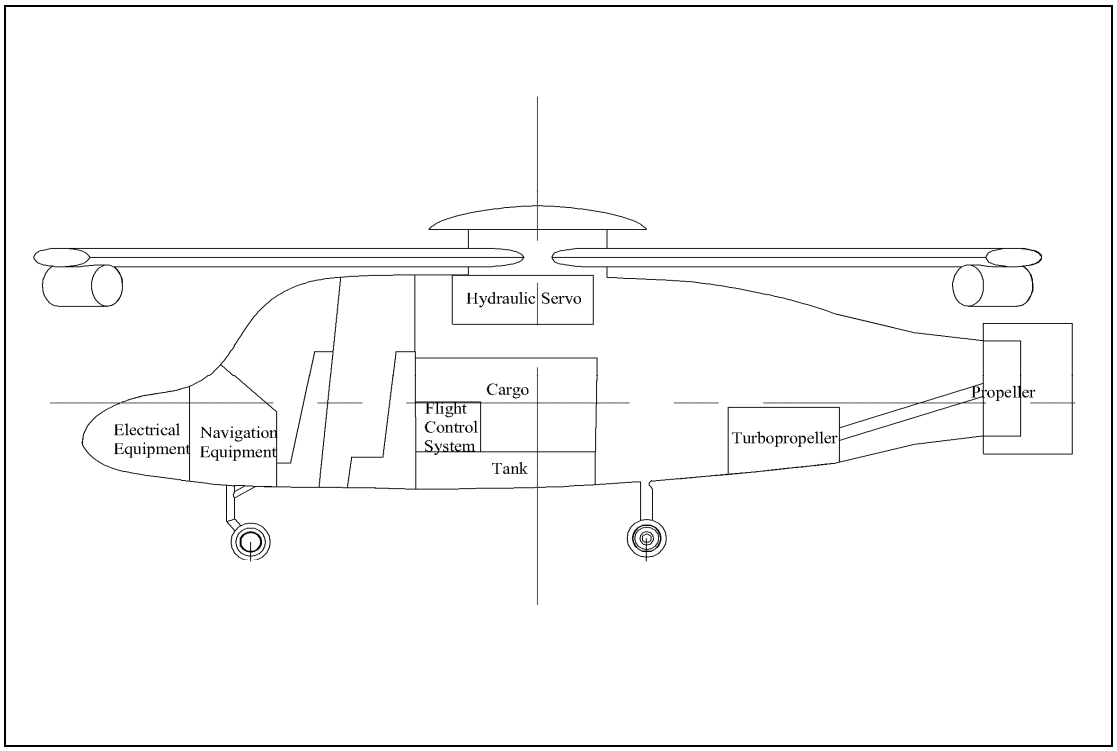

Figure 3.4 Arrangement for Helicopter

3.5 Determination of Barycenter

The location range of barycenter is limited by some factors. In a variety of flight conditions, the helicopter could keep balance by normal control, the volume of rotor blades waving would not exceed the design limitation, and the fatigue strength of blade, hub, and rotor shaft should not exceed design constrains. According to general arrangement of the helicopter, the location of barycenter is determined as in Figure 3.5 and in Table 3.2.

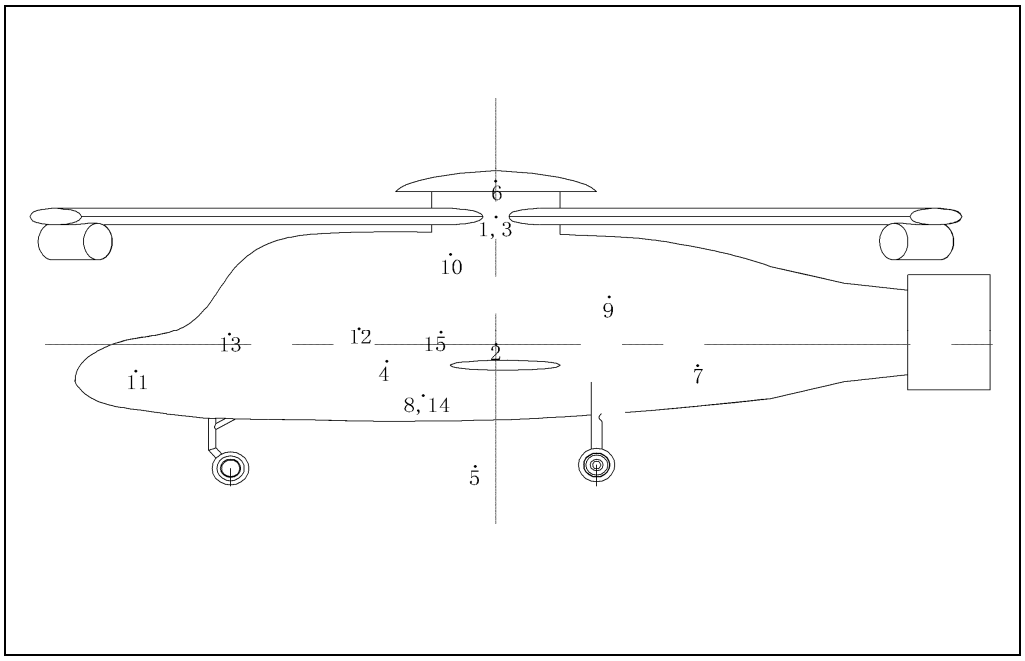

Figure 3.5 Location of Barycenter

Table 3.2 Details about Barycenter

Name	SA365N/kg	Number	Name	New Helicopter/kg	X/m	Y/m
Rotor System	248.5	1	Rotor System	338	0	1.55
Fuselage	517	2	Fuselage	400	0	0
Horizontal and Vertical stabilizer	21	3	Tip-Rocket Engine	21.15*4	0	1.55
Flight Control System	56	4	Flight Control System	55	-1.2	-0.2
Undercarriage	133	5	Undercarriage	130	-0.23	-1.25
Fairing	49.5	6	Fairing	50	0	1.76
Engine	278	7	Turbopropeller	480	2.2	-0.24
Transmission Parts	287.5	——	Transmission Parts	——	——	——
Fuel System	63	8	Fuel System	50	-0.8	-0.6
Static oil	2.5	9	Static oil	2	1.23	0.6
Hydraulic Servo	42	10	Hydraulic Servo	40	-0.5	1.1
Electrical System	104	11	Electrical System	100	-3.92	-0.31
Internal Decoration	118	12	Internal Decoration	100	-1.5	0.21
Auxiliary driving and navigation equipment	25	13	Auxiliary driving and navigation equipment	25	-2.91	0.13
Fuel	1026	14	Fuel	1260	-0.8	-0.6
Payload	879		Payload	890	-0.6	0.16
Empty Weight	1945		Empty Weight	1854.6	0.16	0.25
Total Weight	3850		Total Weight	4000	-0.31	0.04

Chapter 4 Rotor System Design

4.1 Rotor Aerodynamics Shape

The Rotor system is a key system of helicopter, which provides lift force and thrust force for the helicopter. The performance of the helicopter depends directly on rotor. So the rotor system should be designed with a high lift capacity, consuming less power, and there is no excessive vibration or load in all cases.

(1) Airfoil

When the flight speed of helicopter reaches 280Km/h, the rotor will be fixed to stop rotating, and it keeps on flying in the airplane flight mode. So the Elliptical airfoil was used as shown in Figure 4.1. Its leading edge and trailing edge are completely symmetrical. The thickness/width ratio is $b/a = 15\%$. The lift curve, drag curve and polar curve of the Elliptical airfoil are shown in Figure 4.2, Figure 4.3 and Figure 4.4, respectively.

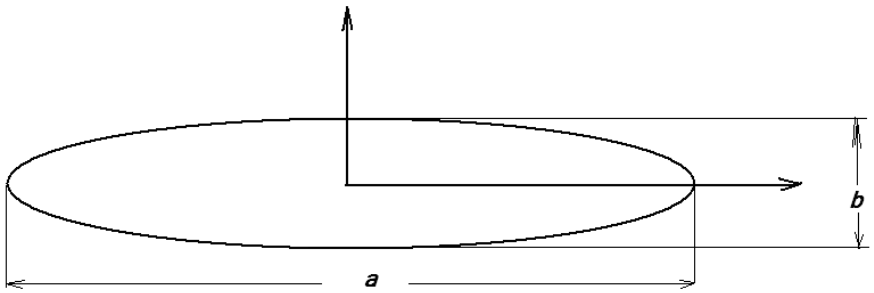

Figure 4.1 Elliptical Airfoil

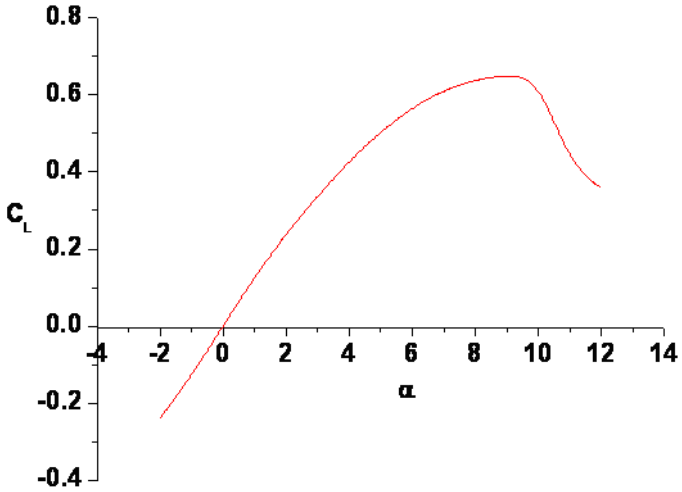

Figure 4.2 Lift Curve of Elliptical Airfoil

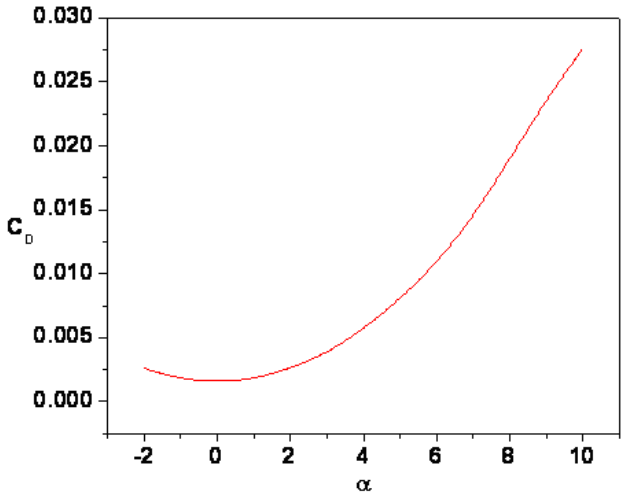

Figure 4.3 Drag Curve of Elliptical Airfoil

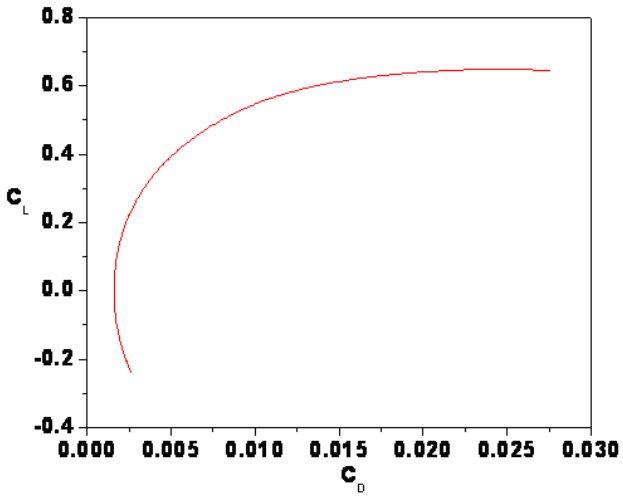

Figure 4.4 Polar Curve of Elliptical Airfoil

(2) Aerodynamic loads of Blade

It is very important to calculate the structural strength of blades in the static stage, the blades which were checked and verified to meet the request can be eligible. Before it, the load calculation should be done first. But load calculation is very complicated, the load changes with time. To simplify the calculation of the load, one condition was considered as the helicopter flies at the speed of 280km/h, and the induced velocity was distributed evenly. This assumption does not bring large errors.

(a) Induced velocity in hover: $\overline{\upsilon}_{10} = \sqrt{\frac{9.8G}{2\pi R^2 \rho}} \Big/ \Omega R = 0.054$

(b) Flap angle: $\beta = 0.0319 - 0.1166\cos\psi - 0.0142\sin\psi$

(c) Induced velocity of forward flight: $\overline{\upsilon}_1 = \frac{\overline{\upsilon}_{10}{}^2}{\overline{V}_0} = 0.00824$

(d) Relative air speed: $W_x = 36.7r + 77.8\sin\psi$, $W_y = -2.73\cos 2\psi - 0.55\sin 2\psi$

(e) Aerodynamic load: $\frac{dT}{dr} = \frac{1}{2}\rho_0 C_{l\alpha}(\varphi W_x^2 - W_x W_y)b$

$$\frac{dT}{dr} = 529r^2 + 2244r\sin\psi + 2379\sin^2\psi + 300r\cos 2\psi + 60r\sin 2\psi + 636\sin\psi\cos 2\psi + 129\sin\psi\sin 2\psi$$

(f) The maximum aerodynamic load in a cycle for calculating the static strength is

$$\frac{dT}{dr} = 529r^2 + 1950r + 1762 \tag{4.1}$$

4.2 Structural Design of Rotor Blades

(1) Structural Arrangement of Blade

One of the main tasks in the preliminary design stage is to select suitable structural form of blade, which determines the basic structure, dynamics and some other design features. In this design, the helicopter will fly in the type of airplane, so there is a hollow beam in the middle of the blade and foam filler on both sides of the hollow beam. At the same time, the center of gravity and the stiffness center are both located in their geometric center. The main dimensions don not change along the radial direction. Figure 4.5 shows the cross section of blade. The geometric parameters are $b = 0.9m$, b_L=0.3*m*, *e*=5*mm*.

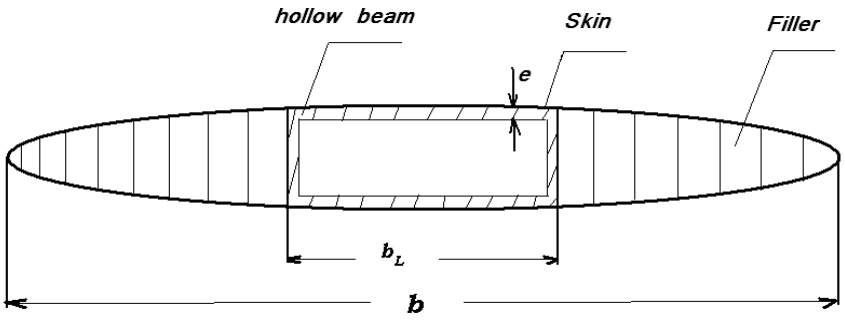

Figure 4.5 Cross Section of Blade

(2) Blade Materials

Here is the ply design of the skin, the layers present from the outmost surface inward are: E glass fiber prepreg cloth 2, high strength carbon fibers prepreg cloth and E glass fiber prepreg cloth 1. The performances of these materials are showed in Table 4.1.

Table 4.1 Blade Materials

Parts	Materials	Ply Direction /°	Density /(g/cm^3)	Elastic Modulus / GPa	Shear Modulus / GPa	Tensile Strength /MPa
Beam	high strength glass prepreg zone	0	1.95-2.10	54±5%	≈4.0	≥1350
Skin	high strength carbon fibers prepreg cloth	±45	1.45-1.55	≈12.5	≈25.0	≥150
Skin	E glass fiber prepreg cloth 1	±45	1.60-1.65	≈13.0	≈13.0	≥160
Skin	E glass fiber prepreg cloth 2	0	1.60-1.65	≈18.0	≈3.0	≥300
Filler	Foam	/	0.05	0.02	0.03	/

(3) Dynamic Properties

The dynamic properties of the blade such as frequencies, mode shape and resonance map were calculated. The first two flap frequencies are $\omega_{\beta 1} = 1.83\Omega$ and $\omega_{\beta 2} = 7.39\Omega$. The first four mode shape of non-rotating blade and the resonance map in flap plane of blade are shown in Figure 4.6 and Figure 4.7, respectively.

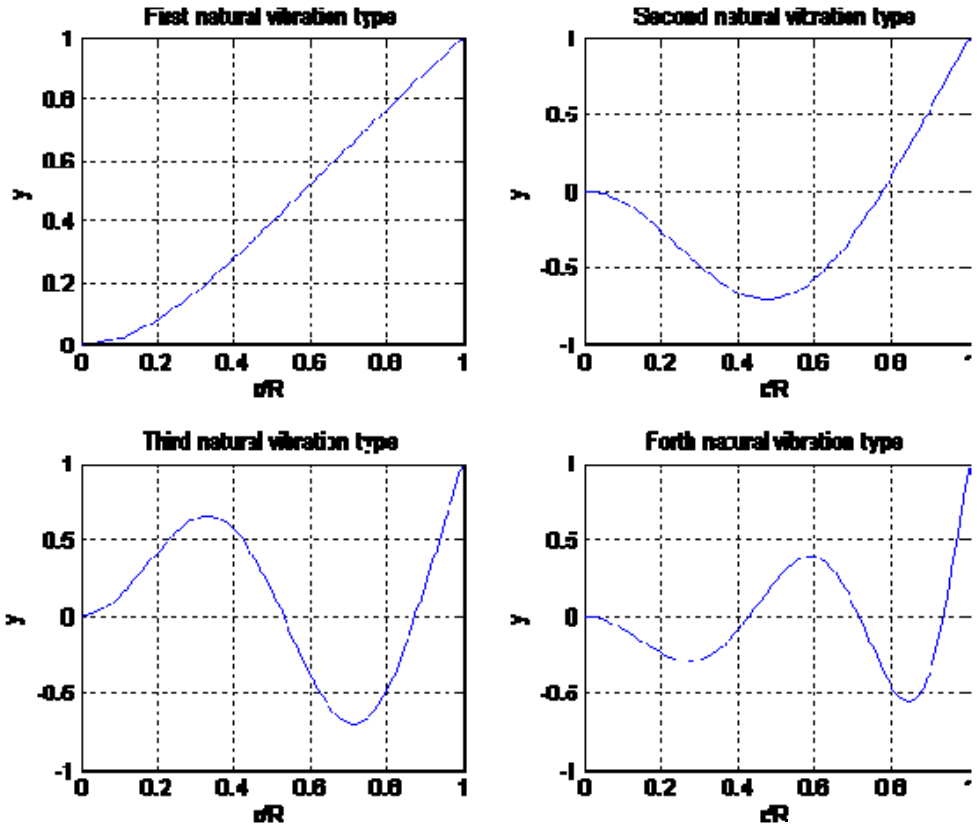

Figure 4.6 First Four Mode Shape of Non-rotating Blade

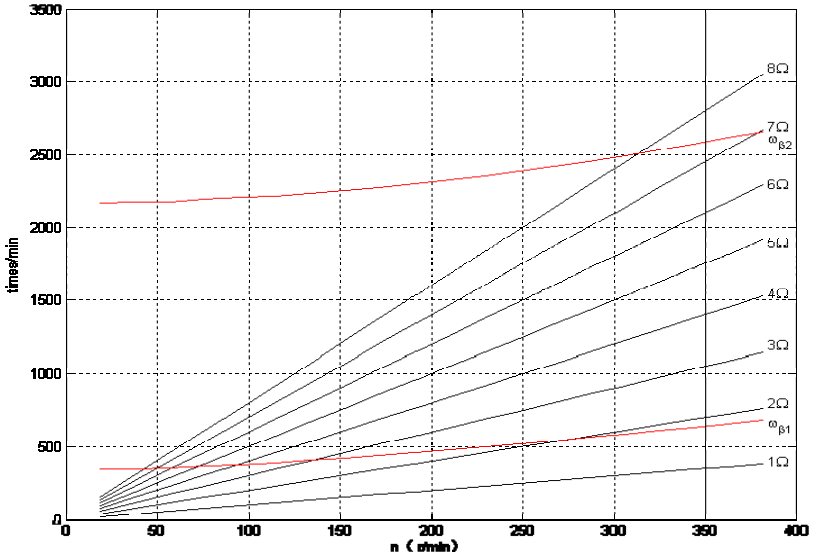

Figure 4.7 Resonance Map in Flap Plane of Blade

(4) Strength of Blade

There are moment, shear force, centrifugal force and torque in the flap and lag of each cross section of rotor blades. The stress produced by shear force and torque has a little effect on the static strength of the blades. Only centrifugal force, flap moment and lag moment were considered.

As an initial approximate calculation, the maximum aerodynamic load in a period at the maximum forward speed was selected for calculating the static strength, and the centrifugal force was in normal speed.

Rotor blade can be seen as a slender beam, the dangerous section should be based on load and the cross sectional stiffness. Here, the strength of the main hollow beam was calculated. Because the lag stress was less, it was ignored. Then the approximate formula was used as

$$\varepsilon = \frac{F}{EA} + \frac{M_y z}{EI_y} \tag{4.2}$$

After analysis and estimates, the blade root is the most dangerous section. So the strength of the blade root was calculated. The flap moment produced by aerodynamic force in arbitrary sections is

$$M_y = \int_r^R \int_r^R \frac{dT}{dr} drdr \tag{4.3}$$

Substituting equation (4.1) into equation (4.3), the flap moment is $M_y = 5 \times 10^5 N \cdot m$. After calculation, the parameters were obtained as $z = 0.0675m$, $I_y = 2.84 \times 10^{-5} m^4$ and $A = 0.0043m^2$.The centrifugal force in the blade root produced by the blade and blade tip jet was $F = 4.3439 \times 10^5 N$. According to Table4.1, the elastic modulus and tensile strength of the hollow beam were $E = 54GPa$ and $\sigma_b \geq 1350Mpa$. After calculation, the maximum stress of the blade was obtained as $\sigma_{\max} = 1289.8MPa < \sigma_b$. It can be seen that the blades can meet the strength requirements.

4.3 Bearingless Rotor

(1) Hub Design of Bearingless Rotor

Using the bearingless rotor can simplify the hub structure, reduce the hub weight, and improve the performance of helicopter, as well as easy-repairing. The cross structure of bearingless rotor hub is shown in Figure 4.8. There are two cross flexural beams connecting the blades.

(2) Rotor Brake

When the speed of helicopter reaches 280Km/h, the rotor would be fixed to stop rotating, and it keeps on flying in airplane flight mode. The rotor and small wings provide lift while the propeller in the tail of helicopter provides thrust force for forward flight. So a brake is needed to design. Referring to the brake system of SA365N helicopter, a brake was designed to be shown in Figure 4.9 and Figure 4.10.

It can be seen from Figure 4.10 that manipulating the handle 7, the friction plate 2 will stop the friction disc 1 to rotate. At the same time, the small gear stops rotating. In the design, the brake will be placed at the phase angle $\psi = 45^0$, while the disc in the rotor shaft with a small part of gear will be placed underneath a blade. When braking, the small gear stops rotating and the rotor shaft continues to rotate until the blade reaches the phase angle $\psi = 45^0$. Thus 4 blades are fixed at the phase angle $\psi = 45^0, 135^0, 225^0, 315^0$, then the helicopter will fly in airplane flight mode.

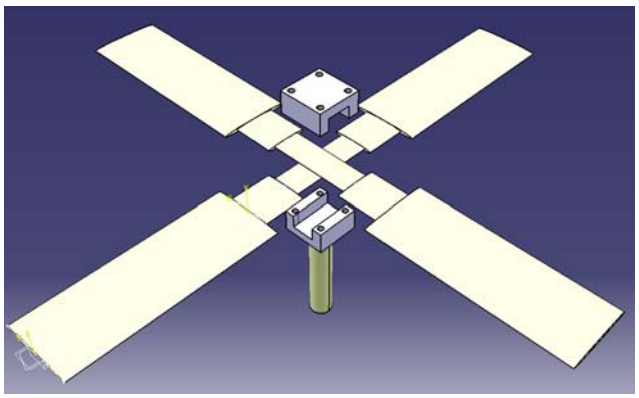

Figure 4.8 Bearingless Rotor Hub

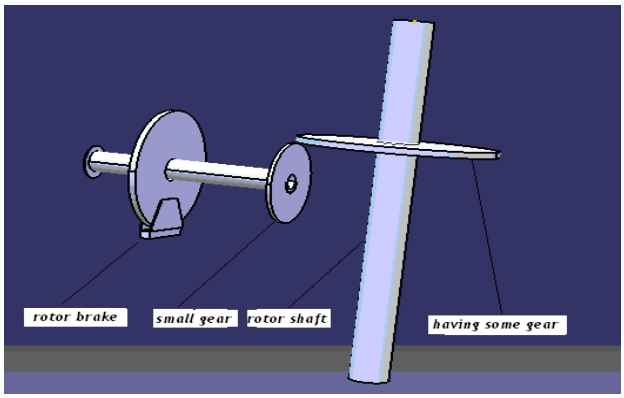

Figure 4.9 Rotor Brake

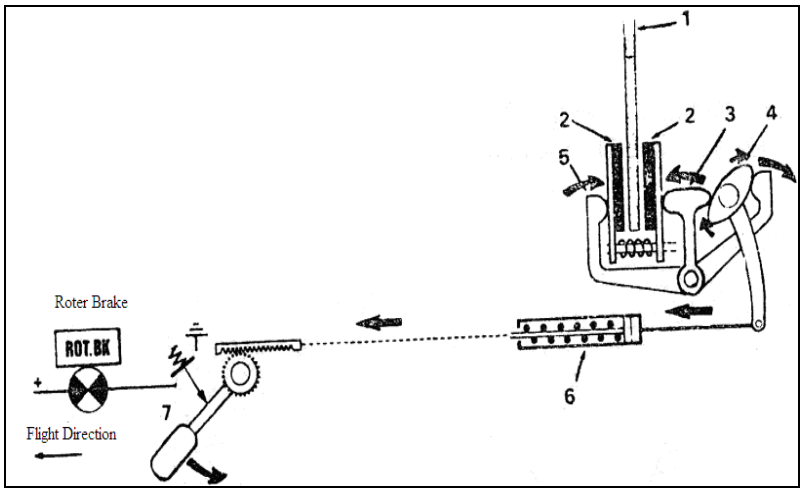

Figure 4.10 Rotor Brake of "Dolphin" Helicopter

(3) Manipulation requirements

The trailing edges of retreating blades must turn to be the leading edges of wings when the rotor is fixed, so that the left and right blades can produce the same lift force for airplane flight mode.

Specific manipulation is as follows: (a) make the collective pitch of all blades equal to zero; (b) controlling the cycle pitch; (c) pulling the cyclic pitch control stick back to upraise both of the leading edges of the advancing blades and the trailing edges of the retreating blades.

Chapter 5 Blade Tip Jet System

5.1 Solid Rocket Engine

The solid rocket engine was used to the blade tip jet system. Obviously, solid rocket engine has got a simple structure as there are no such turbine and compressor equipment in this kind of engine. Therefore, it seems lighter than others and can work effectively in the tough situation of strong centrifugal force. Also, it has got a high thrust-weight ratio. What is the most important is that fuel might not have to be conduced from body to blade tip in that solid propellant is in the combustion chambers.

Solid rocket engine itself has got some disadvantages. Currently, solid rocket engine can not last for a very long time. It is not very convenient to control variation of thrust or repeated start. Some new methods were adopted to solve these problems.

5.2 Parameters of Solid Rocket Engine

(1) Engine Thrust

According to required power of helicopter rotor, the thrust of each blade tip was calculated. As it mentioned before, we know that maximum power of rotor for helicopter to hover is $N_{\max} = 850KW$. Also, when helicopter is in flight forward with a high speed, the rotor will be stopped rotating. At this moment, rotor power will reach its minimum $N_{\min} = 350KW$. Hence, the variation of engine thrust can be determined by empirical formula, velocity of blade tip $\Omega R = 220m/s$ and numbers of blade $k = 4$. Therefore, the maximum and minimum thrusts of each blade tip are $F_{\max} = N_{\max}/(k\Omega R) = 966N$ and $F_{\min} = N_{\min}/(k\Omega R) = 398N$. Apparently, the engine should provide thrust more than 966N and could vary from 398N to 966N.

(2) Engine Specific Impulse

The type of propellant serves as the most significant factor which can influence the engine specific impulse. Also, the size of combustion chambers, functioning procedures of engine and height where engine stays are all related with engine specific impulse. For calculating convenience, the average engine specific impulse was assumed as $I_{sp} = 160000Ns/kg$.

(3) Engine Working Pressure

Engine working pressure is the very combustion chambers pressure. It can be determined by following factors.

(a) To ensure that propellant could combust sufficiently, $P_{eq\min} \geq P_{er(-T^{\circ}c)}$. Usually, its critical pressure varies from 4 to 6 *Mpa* when the double-based propellant engines were used. On the

other hand, it will vary from 2 to 3 *Mpa* as compound propellant engines. We decide to use double-based engines and determine its critical pressure as 4 *Mpa*.

(b) To enhance weight specific impulse as high as possible. Because specific impulse enhances little with pressure increasing the double-based engines were adopted, it makes weight of engine low down little with pressure increasing. Therefore, the lighter the weight of engine is, the closer the critical pressure and optimal working pressure will be. We determine that engine working pressure $P = 4 \times 10^6 Pa$.

According to empirical formula, the maximum working pressure is $P_{\max} = 6 \times 10^6 Pa$.

(4) Engine Nozzle Expansion Ratio

Normally, the first level nozzle expansion ratio of solid rocket engine varies from 7 to 10. Here we use the nozzle with an expansion ratio $\varepsilon_A = 8$.

5.3 Engine Component Design

The required power and engine thrust will decline with increasing of helicopter flight forward speed. Thereby, engine should not only provide big enough thrust in order to lift up the helicopter, but also thrust can be varied randomly. Even sometimes helicopter needs to work with hover status for a long time, which will cast a challenge to engine to stop and restart repeatedly. However, it is not a big case for a solid rocket engine to provide this big enough thrust. Therefore, our design focuses on how it could vary its thrust and start repeatedly.

(1) VTAE

A new type solid engine—VTAE (Variable throat area engine) was adopted as shown in Figure 5.1. The design of VTAE was aimed to solve the problems of thrust variation and repeated start of solid engine.

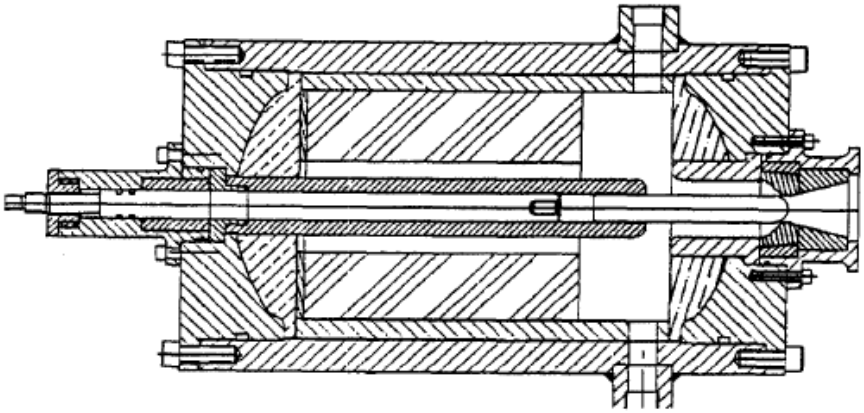

Figure 5.1 Variable Throat Area Engine

As shown in Figure 5.1, the pintle was assembled in the supporting sets of combustion chambers and drive it move toward and backward by hydraulic system to vary throat area.

According to balance pressure formula $P_c = \left[\rho_p caA_p / A_t\right]^{\frac{1}{1-n}}$ and thrust formula $F = C_F P_C A_t$. The engine thrust was merely varied by regulating throat area A_t. When thrust increases to maximum, the throat area becomes minimum. Simply, when thrust decreases to minimum, the throat area becomes maximum. Additionally, as mentioned before, engine will stop working as engine minimum working pressure is lower than critical pressure, which can just meet the requirement of repeated stop. Theoretically, the propellant of high burning rate pressure index should be choosen (n=0.7~0.9) in order for large range of thrust variation. n=0.7 was choosen.

(2) Engine Combustion Chamber

(a) Engine combustion chamber size

The steel was used as shell materials with metal cylinder structure. This kind of structure is very simple and mature in manufacture. Also there are not many joints, which could be better fit in complicated aerodynamic situation and centrifugal force. Typically to solid engines, diameter of engine is combustion diameter. According to optimal structure weight, engine diameter may be decided by next steps. The combustion chamber was simplified to a cylinder with plats of both of two sides. At the tail of combustion chamber, there is a ventilation, whose area is A_p. The Engine structure weight is

$$m_c = \frac{\varphi P_{\max} \rho_m}{[\sigma]} \left(\frac{2\pi R^2 V_p}{\pi R^2 - A_p} + 2\pi R^3 - A_p R \right) \tag{5.1}$$

where, m_c is the function of *R*. So there must be optimal diameter which makes combustion chambers lightest. Derivate equation to R could obtained

$$(6\pi R^2 - A_p)(\pi R^2 - A_p)^2 = 4\pi R A_p V_p \tag{5.2}$$

By equation (5.2), the optimal diameter *R* can be obtained through V_p and A_p. blade tip maximum thrust *F*=966 *N*, engine working duration *T*=40 *min*, engine propellant specific impulse I_{sp}=160000 *Ns*/*kg*, propellant density $\rho_p = 1.7 \times 10^3 kg/m^3$. Assuming that engine will work with full power about 40 minutes, then weight of propellant $M_p = FT / I_{sp} = 14.50 Kg$, volume of propellant $V_p = M_p / \rho_p = 8.52 \times 10^{-3} m^3$. The area of ventilation A_p can be approximately equal to nozzle throat area. Because engine thrust varies from 398*N* to 966*N* and throat area reaches maximum when thrust decreases to minimum. Therefore, the area of ventilation must be a little bigger than throat area of minimum thrust. $A_p = 70 \times 10^{-4} m^2$ was selected as the initial area of ventilation. Thrust coefficient is $C_F = 0.0153$. So when engine thrust reaches its minimum

value $F_{\min} = 398N$, throat area is $A_t = 65 \times 10^{-4} m^2$. Hence, the optimal radius value was $R = 0.09m$ with which the weight of combustion chamber is the lightest. The optimal length-radius ratio is $\lambda = L/R = V_p/[(\pi R^2 - A_p)]R = 5.14$. Apparently, the length of combustion chamber is $L = 0.462m$.

(b) Thickness of combustion chamber shell

According to empirical formula, the minimum thickness of cylinder is $\delta_{\min} = \varphi p_{\max} D/2\xi[\sigma]$. If the steel or aluminum is used as shell materials, the formula can be simplified as follows $\delta_{\min} = \varphi p_{\max} D_i/(2.3\xi[\sigma] - \varphi p_{\max})$. Considering the pressure variation from deviation of throat size, $\varphi = 1.1$, ξ=0.9, then $\delta_{\min} = 8.9 \times 10^{-4} m$. Taking the safe coefficient *n*=1.2, then it can be got $\delta_t = 4mm$.

(c) Engine shell weight

As mentioned before, the engine size is determined by optimal structure weight. After calculated the appropriate size, the combustion chamber weight m_c can be calculated by equation (5.1) $m_c = 2.18kg$.

(3) Nozzle

(a) Nozzle size

The size of nozzle as shown in Figure 5.2 might be calculated after expansion ratio being determined. Here $\varepsilon_A = 8$. The outlet area of nozzle A_e can be estimated by the awareness of throat area and expansion ratio $A_e = 8A_t = 5.6 \times 10^{-2} m^2$. Then radius of nozzle outlet is $R_e = \sqrt{A_e/\pi} = 0.133m$. Expansion angle $\alpha = 15^\circ$, Through the simple geometric formula $sin\alpha = (R_e - R_t)/L$, the length of nozzle is $L = 0.33m$. Typically, the thickness of nozzle shell can be determined by the same way with combustion chamber. The alloy steel - 40MnB was taken as nozzle materials, its $[\sigma] = 981Mpa$. Therefore, the minimum thickness is $\bar{\delta}_{nmin} = 8.67 \times 10^{-4} m$.

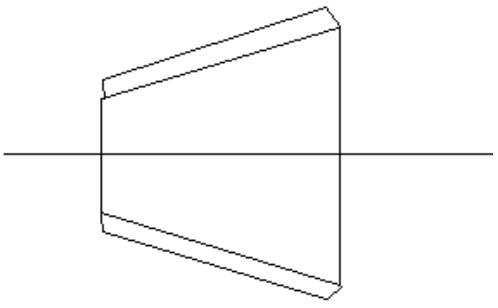

Figure 5.2 Nozzle

(b) Weight of nozzle

The weight of nozzle seems reasonable to be determined by principle of maximum weight specific impulse. On the under-expanded status, the weight of nozzle will grow with increasing of nozzle expansion ratio. There must be an optimal expansion ratio which makes nozzle lightest as total impulse is fixed. The weight of nozzle could be calculated by the following empirical formula. $m_n = \frac{1}{\sin\alpha} A_t(\varepsilon_A - 1)\bar{\delta}_n \rho_n = 1.47kg$.

5.4 Specific Analysis

(1) Engine Thrust Variation Analysis

The engine thrust is $F = C_F P_c A_t$ in which $P_c = [\rho_p caA_p / A_t]^{\frac{1}{1-n}}$. Assuming throat area after variation is A_{t1}, $A_{t1} = \varepsilon A_t$ in which ε is throat area coefficient. Then $F_1 = F\varepsilon^{\frac{1}{n-1}}$, $P_{c1} = P_c\varepsilon^{\frac{1}{n-1}}$. If *n*=0.7, the engine thrust variation with throat area variation is showed in Figure 5.3. When throat area decreases to $A_t = 44\times10^{-4}m^2$, engine thrust can reach the maximum as the rotor need *F*=966*N*. Apparently, engine thrust is 398*N* when throat area is equal to $65\times10^{-4}m$. From Figure 5.3, the variation of throat area is relatively smooth in the process of thrust variation, which indicates that engine thrust variation manageability performances well.

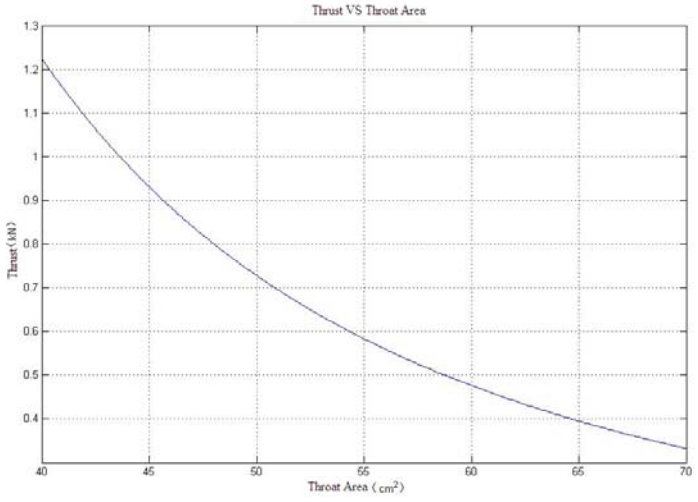

Figure 5.3 Thrust VS Throat Area

(2) Repeated Stop and Restart

As a matter of fact, as throat area is bigger than $70\times10^{-4}m^2$, engine will stop working because combustion chamber pressure is lower than critical pressure. This can perfectly meet the requirement of repeated stop. The engine can restart when repeated ignition is adopted. Therefore, this repeated stop and restart issue will be solved.

(3) Process of Throat Area Variation

A hydraulic propulsion shown in Figure 5.4 may pull or push cone block to change throat area. When the cone block moves forward, throat area becomes small and then engine thrust rises. Oppositely, when the cone block moves backward, engine thrust falls.

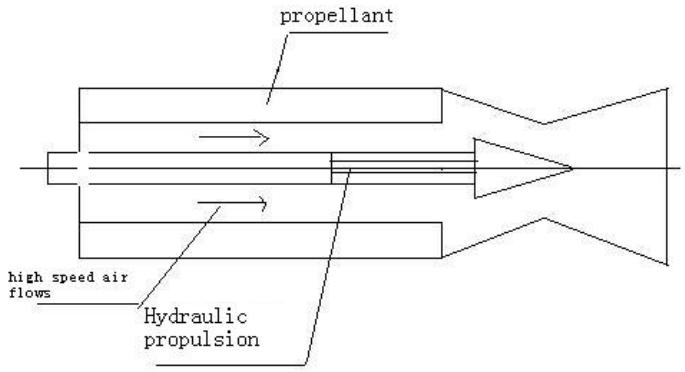

Figure 5.4 Variable Throat Area Engine Structure Sketch

5.5 Other Component Design

Besides the design of combustion chamber and nozzle, there are other many components to be designed and given parameters, for example, ignition system, thrust vector control device and so on. But they do not play a significant part in this design. What is more, they can not affect final engine weight very much. Therefore, some estimation for them was given in order to calculate final engine structure weight. The weight of combustion chamber and nozzle are separately $m_c = 2.18kg$ and $m_n = 1.47kg$. Other parts weight should be controlled to lighter than 2kg. Therefore, weight of engine structure is $m_{\mathrm{m}} = 5.65kg$. Plus weight of propellant, total weight of engine is approximately m=21.15kg.

Finally, the blade tip jet is shown in Figure 5.5.

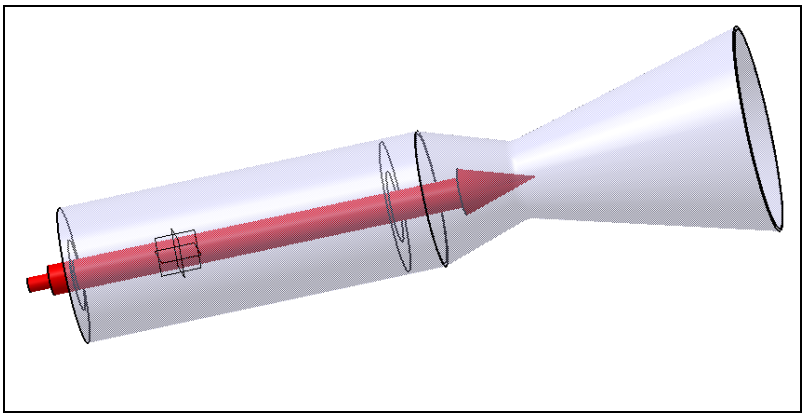

Figure 5.5 Blade Tip Jet

Chapter 6 Vectored Thrust Ducted Propeller System

6.1 Power System Select

Pratt & Whitney Canada PW100 series engines and the Czech company Walter M602 series engines are free dual-rotor turbine turboprop engine, the main parameters of comparison are as follows:

Table 6.1 Main Parameters of PW100 and M602 Series Engines

	Maximum cruise power（kW）	Take-off power（kW）	Take-off Fuel Efficiency [kg/(kWh)]	Width（mm）	Height（mm）	Length（mm）	Weight（kg）
PW 123	1514	1864	0.286	660	838	2134	450
PW 124	1557	1557	0.285	660	838	2134	450
PW 125	1514	1864	0.283	660	838	2134	450
PW 126	1553	1985	0.283	660	838	2134	450
PW 127	1589	2051	0.280	660	838	2134	481
M602A	1200	1360	0.350	753	872	2869	570
M602B	1400	1500	0.303	753	852	2285	490

By comparing, the performance of PW100 series turboprop engines far exceeds the performance of the M602 series turboprop engines, and in the PW100 series , the PW127 in the take-off power and maximum cruise power is greater than the PW123 - PW126, and the take-off Fuel Efficiency is less than the PW123 - PW126. The only shortage is that the PW127 is heavier than PW123 - PW126 engine, such as 30kg, but taking into account compound helicopter's large forward flight speed, the PW127 is still more to meet the requirements, so the PW127, Canada's Pratt & Whitney was selected. The mass distribution of SA365N is shown in table 6.2.

Table 6.2 Mass Distribution of SA365N

Airframe	Rotor system	Landing Gear	Engine	Drive system
517kg	248.5kg	133kg	278kg	287.5kg

It can be seen that the engine and drive system for the total mass of 565.5kg.The Compound helicopter doesn't have turbo-shaft engine and drive system, It will reduce the weight of 565.5kg,but the weight of the engine for the vectored thrust ducted propeller system is 481kg .Because the tail beam is shorten and the tilted tail beam is canceled. Compared with the reference helicopter, the new designed helicopter will have lower weight.

6.2 Aerodynamic Characteristics Analysis

Because the propeller is besieged by the duct, the propeller and the duct form a coupling system, the ducted propeller works under the collecting flow effect of the duct. Ducted propeller

installed in the combinations of propeller and duct with the same working conditions compared to the isolated propeller, there are some particularities as follows:

(1) Under the condition of no tip flow, the gap between the tip and the inner wall of duct body must be smaller(less than 1% of the chord length, is generally level-mm). Due to the existence of inner wall and the duct body has a certain length, the tip vortex of the occurrence and development is blocked, so the ducted propeller no longer have tip vortex with loss of energy and loss of lift.

(2) Changes in wake geometry of the propeller due to the protective effect of the ducted, Airflow through the propeller is a more uniform flow, and as a result of the inner body wall adsorption, the wake will no longer contract. if there is a suitable expansion angle in the ducted design, and even its wake will have some expansion.

(3) Ducted is the lifting body, it generates propulsion, ducted body is formed by the airfoil, and the equivalent for the ring wing. Well-designed shape ducted body, using a special configuration of the leading edge, air flow in the ducted body, it will have a forward direction force.

In the same rotational speed, the thrust of ducted propeller system is greater than the thrust of the propeller in isolation. And with the rotation speed, ducted propeller system, the relative isolation of the propeller thrust increment also increased, up to isolate the incremental thrust about 42%. When the horizontal and vertical control surface do not tilt, the rudder face will not have airflow obstruction effect on the vectored thrust ducted propeller system.

At different speed, when the level control surface fixed by the different angles and the absolute value of the angle of the vertical control surface increases, the thrust of vectored thrust ducted propeller system decreases, because of the vertical rudder surface's deflection, the airflow of the system is blocked, and thrust reduces. In addition, as the rotational speed increased, the blockage of the vertical rudder surface become more obvious .The deflection of the level control surface has a small airflow obstruction effect on the vectored thrust ducted propeller system.

6.3 Vectored Thrust Ducted Propeller System Design

(1) Propeller Design

Table 6.3 Performance of Ducted Propeller Design

Design Power	300kW
Rotation Speed	1200rpm
Blade Radius	0.75m
Blades Number	5
Advance Ratio	3.52
Power Coefficient	4.03
Thrust Coefficient	2.57

Design Thrust	650kg
Efficiency	0.692

Table 6.4 Geometry Size of Propeller

Airfoil	Clark-Y
Blades number	5
Chord	15mm
Negative twist	25°
Axial location	150mm
Diameter	1.5m

(2) Ducted Body Design

(a) Analysis of ducted thrust

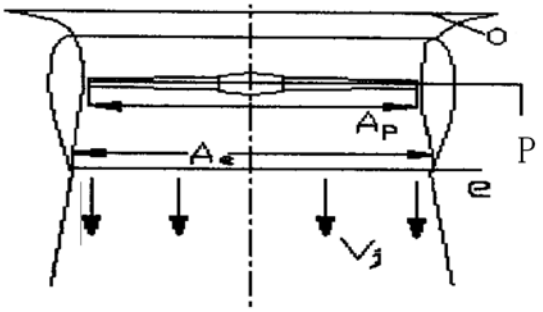

Figure 6.1 Vertical Ducted Propeller Sketch

For a vertical ducted propeller, the equation of ducted thrust can be obtained by the energy equation,

$$\frac{T}{HP} = \frac{1100}{V_j} \tag{6.1}$$

Where, the constant 1100 was derived from Imperial units. The unit of thrust is lb, unit of speed is ft / s, the power unit is horsepower, and thrust can be expressed as:

$$T = \rho A_e \left(\frac{1100}{T / HP} \right)^2 \tag{6.2}$$

By the Bernoulli equation, the pressure equation can be obtained,

$$P_0 + \Delta P_r = P_j + \frac{1}{2}\rho V_j^2 \tag{6.3}$$

Due to $P_0 = P_j$,

$$\Delta P_r = \frac{1}{2}\rho \left(\frac{1100}{T / HP} \right)^2 \tag{6.4}$$

The propeller thrust is $F_r = \Delta P_r A_p = \frac{1}{2}\rho\left(\frac{1100}{T/HP}\right)^2 A_p$. For the entire ducted propeller system, the momentum equation is

$$F_{duct} + F_r = mV_j = \rho A_e V_j^2 \tag{6.5}$$

$$F_{duct} = \rho A_e V_j^2 = \frac{1}{2}\rho A_p V_j^2 \tag{6.6}$$

By equation (6.5) and (6.6), the following equation is obtained

$$\frac{F_{duct}}{T} = 1 - 0.5\frac{A_p}{A_e} \tag{6.7}$$

The Figure 6.2 gives the curves compared with the experimental curve. For the sake of convenience, the area ratio in the figure is the ratio of ducted exit area and propeller disk area. As can be seen from the figure the curves are in the same trend when the ratio between 1.0-1.25. The formula and experimental curves prove that the area ratio is an important parameter which can improve the ducted thrust. Because the ducted has the ability to absorb, even the ducted is in the vertical position, propeller still has some pre-axial initial velocity, and the propeller which has a small initial velocity in this article is in a Horizontal position, as a result of the pumping capacity, it also has the same pre-axial initial velocity, the experimental data in the figure also has a important significance for our design in which initial velocity is not high. According to the analysis above, increasing the ducted exit area suitably is conducive to improving the ducted thrust.

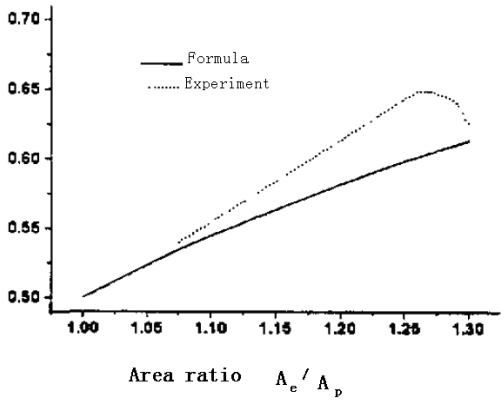

Figure 6.2 Calculational VS Experimental Results

(b) Airfoil select and length design of the ducted

In the ducted design, in order to ensure the area ratio, we should choose the airfoil which has a large relative coordinates under the surface, such as CLARK YM-18, NACA 2418, NACA 2421,

NACA 2424, NACA 23021 and so on. In addition, the radius of ducted lip and the expansion angle have a greater impact on the performance of the ducted. The airfoil was selected according to flat lumen、bend、round head、large thickness and with the expansion.

Airfoil CLARK YM-18 was selected. CLARK YM-18 for the maximum thickness is 17.98 percent the chord length, 30.2 percent in the position of the chord length; maximum curvature for the 3.55% chord length, 40.2 percent in the position of the chord length, airfoil leading edge radius of 2.9% value of the chord length, the thickness of the rear airfoil chord length of 0.1800 percent.

Figure 6.3 CLARK YM-18 Airfoil

Then according to the area ratio and the known airfoil data, the ducted length can be identified by the following formula,

$$\frac{C_{duct}(y_e - y_{\min})}{100(R+\delta)} = \sqrt{\frac{A_e}{A_g}} \tag{6.8}$$

Where, R represents blade radius, δ represents the gap between propeller tip and the ducted, y_e represents relative coordinates of ducted outlet diameter, $y_{\min}$ represents relative coordinates of the smallest diameter of ducted cross-section, we can get these two values from the data of the airfoil. A_e / A_g represents the ratio of the ducted effective exit area and geometric area.

In addition, ducted itself in this system is to eliminate the wake contraction of the slipstream through the ducted. The ducted propeller can get more air to improve its aerodynamic efficiency. The existing experimental results show that: when the ducted is shorten, the ducted propeller thrust will decline. As Shown in Figure 6.4, C/D is between 0.8 to1.0, the thrust ratio has been close to 1.

The tip gap also has a big effect on the performance of the ducted propeller as shown in Figure 6.5. The value of the gap size was analyzed. The follow figure is the relationship of thrust ratio and the tip value. And in the figure δ represents the ratio of the distance between propeller tip and ducted inner wall and the radius of the ducted. It can be seen from Figure 6.5, with increasing distance between propeller tip and ducted inner wall, the thrust of ducted propeller system will be reduced. So in the actual design of the project, we should pay more attention to the gap value, and the gap value should be reduced as much as possible.

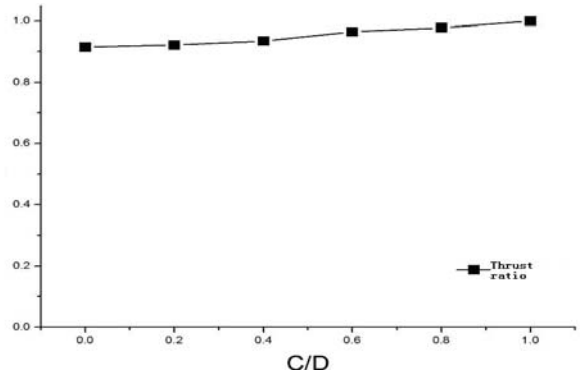

Figure 6.4 Effect of Duct Length on Thrust Ratio

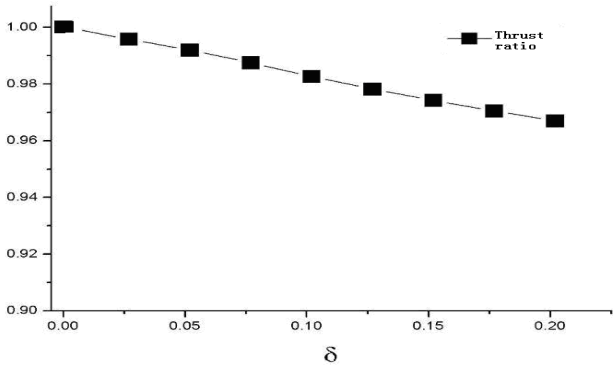

Figure 6.5 Effect of Tip Gap on Thrust Ratio

Table 6.5 Ducted Design Results

Propeller Power	Propeller Radius	Ducted Airfoil	Area Ratio	Tip Gap	Ducted Length	Ducted Exit Radius	Ducted Thrust
300kW	750mm	CLARK YM-18	1.2	10mm	740mm	821.6 mm	601.0kg

(c) Horizontal rudder and vertical rudder design

According to engineering requirements, the yaw and pitch of helicopter need to control by horizontal and vertical rudder. Table 6.6 lists the parameters.

Table 6.6 Main Parameters of Horizontal and Vertical Rudders

Part Name	Parameters	Size
Horizontal Rudder	Chord	20mm
	Number	1
	Airfoil	NACA 0012
Vertical Rudder	Chord	28 mm
	Number	3
	Airfoil	NACA 0012

Finally, the 3D view of the vectored thrust ducted propeller is shown in Figure 6.6.

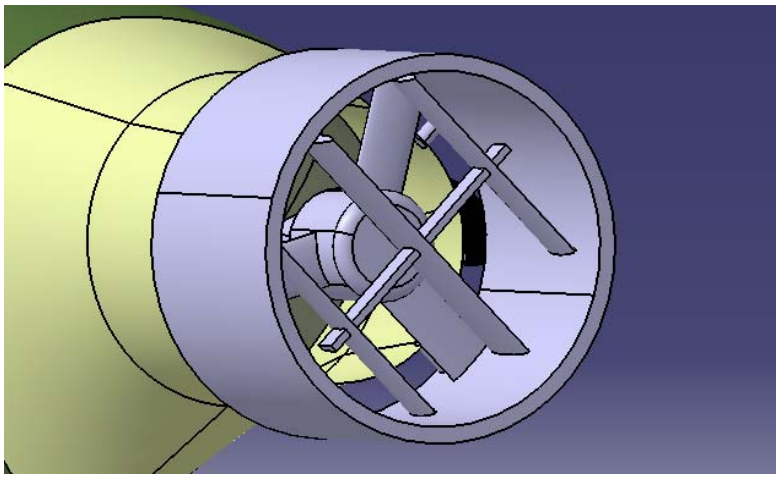

Figure 6.6 Vectored Thrust Ducted Propeller

Chapter 7 Fuselage Structural Design

7.1 Airframe Structure

As a medium-sized helicopter with a total weight of only 4000kg, considering the reduction of flight drag and weight efficiency, its airframe structure was finally designed as thin-walled structure because of pithiness of thin-walled structure、high weight efficiency and simple maintenance. The outline of the helicopter is shown in Figure 7.1.The structure may be made by using light composite materials to reduce the weight and meet the requirements of strength.

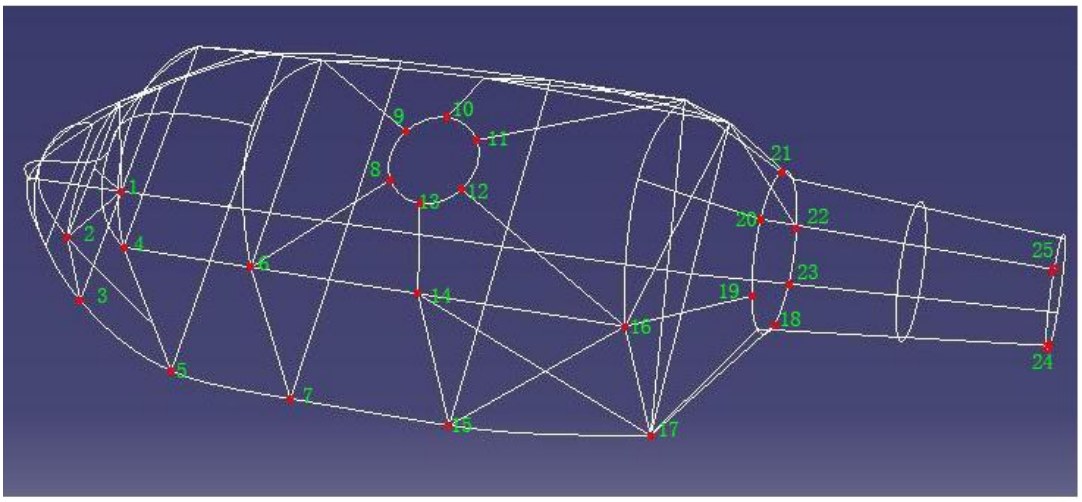

Figure 7.1 Outline of Helicopter

The downwash force acts on the skin. The form of pressure passed on to the truss which connected with the skin. Then transferred to the points 4、5、6、7、14、15、16、17 and the points which are on the vertical symmetry plane of the helicopter. At last the pressure delivered to the body. The front flow acts on the windscreen and the skin, the pressure passed on to the truss which connected with the skin. Then delivered to the points 2、4 and the points which are on the vertical symmetry plane of the helicopter. The drag acted on the rotor through the rotor shaft spread to the points 8、9、10、11、12、13,then transferred to the body. Landed on the ground, ground supportiveness from the undercarriage acts on the points 1、17,then it's transmitted upwards to the fortified box. The weight of tank and astronautic electric insulations according to the points 15、17 which are connected with the tank,and truss is transmitted upwards, onwards to the airframe. The weight of cabinet planking and passenger is transmitted to the points 7、15 then delivered to the body.

7.2 Overload Landing Analysis

In order to check the helicopter landing in a variety of different circumstances if it is safe to the strength of the landing gear in all cases can meet the strength requirements of stiffness, there is a need for analysis of the landing load.

(1) Overload coefficient

Table 7.1 lists the biggest load of the form factor. According to the data in the form the largest load factor n = 3 was taken.

Table 7.1 Largest Coefficient Used by Different Countries

Country	name of norms	year	biggest overload
USA	MIL-8689	1954	2.3～3.5
USA	CAM-7	1962	2～3.5
USA	FAR 29	1971	2～3.5
USA	Strength of norms	1955	3～4
Soviet Union	Strength of norms	1962	2.5～3
UK	BCAR,G part	1966	2～3

(2) Parked load calculation

The helicopter was designed to use wheel landing gear. The maximum take-off weight of helicopter is 4000 kg. The overload coefficient is 3. The size of the landing gear is shown in Figure 7.2. The front landing wheel parked load is $P_{tjq} = GL_2 / L = 1380kg$. The main landing wheel parked load is $P_{tjzh} = GL_1 / 2L = 1310kg$.

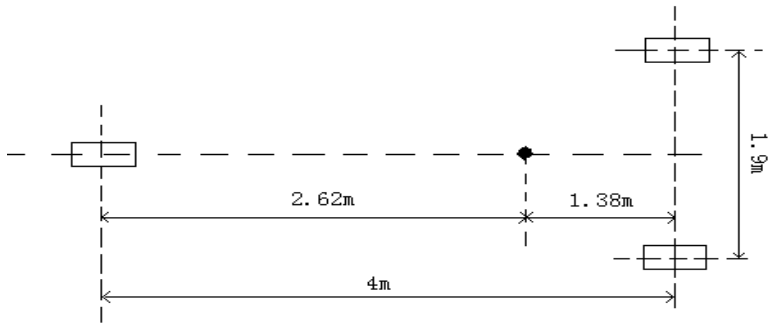

Figure 7.2 Size of Landing Gear

(3) Landing a variety of terms and data

Overload landing generally choose some more serious situations to calculate. The following are some serious situations we should pay attention to. Through searching information, we find

the average coefficient of sliding friction μ is 0.4, and when the wheel sliding to the side, the friction coefficient is between 0.5 and 1.0.The friction coefficient of wheel which close to the sliding side is 0.8, the other wheel's friction coefficient is 0.6. Now the following cases were taken to calculate the load. (1) The helicopter landed with its head bowing, i.e. only front wheel landed. (2) The helicopter landed on the one of its main wheel. (3) The helicopter landed horizontally with its main wheels, but they slid lift or right. (4) The helicopter landed with all wheels but they all slid left or right. (5) The helicopter landed only on its main wheels .Table 7.2 lists the data of every case.

Table 7.2 Landing Load (kg)

Loading location	Front wheel			Left Main Wheel			Right Main Wheel		
Loading cases	P_x	P_y	P_z	P_x	P_y	P_z	P_x	P_y	P_z
1	1656	4140	0	0	0	0	0	0	0
2	0	0	0	0	3930	0	0	0	0
3	0	0	0	0	1965	1179	0	1965	1572
4	0	2070	1656	0	1965	1179	0	1965	1572
5	0	0	0	1572	3930	0	1572	3930	0

7.3 Landing Gear Design

Helicopter landing gear's main role is to absorb energy when it is landing with a vertical speed ,reduce the landing impact caused by overload. In addition, the helicopter landing gear was also used to have a slide on the ground and the ability to roll, and reduce the collision and bumps in the sliding cause by the uneven ground.

(1) The type of landing gear

There are two types of landing gear, one is the fixed landing gear, the other is retractable landing gear. The fixed landing gear is often used to low speed helicopter, and we often choose the retractable landing gear on high speed aircraft. Modern aviation aircraft are often taking -off and landing on land, so we often use landing gear with wheels.

(2) The layout and the structure of landing gear

The landing gear not only can guarantee the stability and manage ability, but also can decide the load of it if the layout of landing gear is suitable .There are several types of layout of landing gear ,For example ,before the three-point, after the three-point, bicycle-style, and the fulcrum-style. At present, the most widely used is before the three-point. That is to say the main landing gear is behind the center of gravity, the front landing gear is installed under the nose of helicopter. The before three-point can keep stability when it's rolling, when helicopter landed at

high speed and small angle of attack, The front three-point of can keep the helicopter sliding and avoid "Jump" phenomenon. According to the load bearing and transmission, the landing gear can be divided into Truss-type landing gear, Beam Rack landing gear and the Compound.

(3) Strength checking of landing gear

The 30CrMnSiNi2A was taken as the material of landing gear, its allowable stress $\sigma_b = 1700Mpa$, choosing the most serious loading to analysis the strength of landing gear. It's obvious that landed only on main wheels will be the most serious situation. Figure 7.3 shows the size of landing gear and force analysis of it.

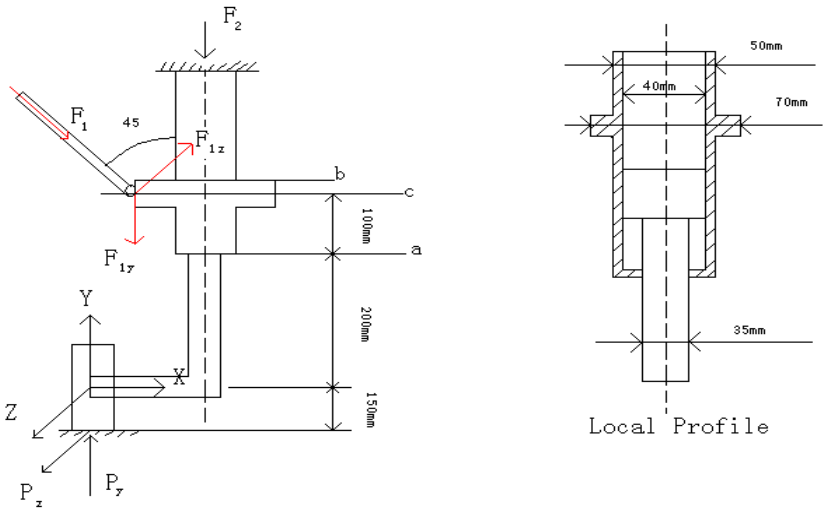

Figure 7.3 Size of Landing Gear and Force Analysis

The ground reaction forces to landing gear are $P_y = 38514N$ and $P_z = 15405.6N$. The balance of force in all directions is $\sum F = 0 \Rightarrow \begin{cases} F_{1y} + F_2 = P_y \\ F_{1z} = P_z \end{cases}$. Then $F_1 = 21786.8N$, $F_{1y} = F_{1z} = 15405.6N$, $F_2 = 23108.4N$. Through simple calculation we can get bending moment diagram and torque diagram of the pillar. Figure 7.4 shows the bending moment and torque of pillar.

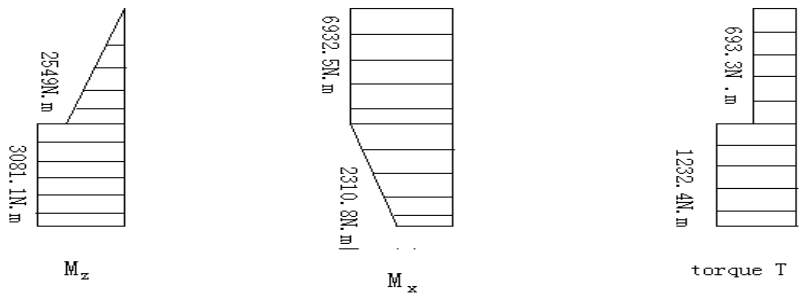

Figure 7.4 Bending Moment and Torque of Pillar

(a) The strength checking for "a" section of the active bar

The active bar has a complicated deformation such as compression, bending and reverse deformation. The third strength theory was used to check the strength. The following equation can be got by the third strength theory $\sigma = \sqrt{(\frac{P_y}{A_1} + \frac{M_1}{W_1})^2 + 4(\frac{T_1}{W_{1t}})^2}$ in which $A_1 = 1.256 \times 10^{-3} m^2$, $M_1 = \sqrt{M_x^{\ 2} + M_y^{\ 2}} = 6209.8 N.m$, $W_1 = 6.26 \times 10^{-6} m^3$, $W_{1t} = 1.256 \times 10^{-5} m^3$. Hence, the active bar meets the strength requirement due to $\sigma = 1019.5 Mpa < 1700 Mpa$.

(b) The strength checking for section "b" of cylindrical body.

The section b of cylindrical body has a compound deformation. The stress is $\sigma = \sqrt{(\frac{F_2}{A_2} + \frac{M_2}{W_2})^2 + 4(\frac{T_2}{W_{2t}})^2}$, $M_2 = 7383.8 N.m$, $A_2 = 7.065 \times 10^{-4} m^2$, $W_2 = 7.24 \times 10^{-6} m^3$, $W_{2t} = 1.45 \times 10^{-5} m^3$. The section b of cylindrical body meets the strength requirements due to $\sigma = 1056.9 Mpa < 1700 Mpa$.

(c) The strength checking for "c" section of cylindrical body.

The section c of cylindrical body has compression, bending and reverse deformation. The stress is $\sigma = \sqrt{(\frac{P_y}{A_3} + \frac{M_3}{W_3})^2 + 4(\frac{T_1}{W_{3t}})^2}$, $M_3 = 7586.4 N.m$, $A_3 = 2.6 \times 10^{-3} m^2$, $W_3 = 3 \times 10^{-5} m^3$, $W_{3t} = 6 \times 10^{-5} m^3$. The section c of cylindrical body meets the strength requirements due to $\sigma = 270.8 Mpa < 1700 Mpa$

(d) The strength checking for oblique pole

Oblique pole is bearing the axial force to be checked by $\sigma = \frac{F_1}{A} = 277.5 Mpa < 1700 Mpa$ which meets the requirement.

7.4 Bulkhead Design of Helicopter

Bulkhead is the main components of thin-walled structure ,not only can it keep the shape ,but also it supports and enhance the shin and stringers .In addition ,bulkhead can join the other parts together ,and it also can fix a variety of devices.

(1) The shape design of bulkhead

The common bulkhead can bear little load ,so use aluminum to make bulkhead round ,the sections of bulkhead are usually "Π" or "Z", where concentrated load or special forces exist we can use enhanced bulkhead to meet the strength requirement. For example, we should use enhanced bulkhead where landing gear is fixed .where engine is placed, the enhanced bulkhead is

also needed .The most difference between common bulkhead and enhanced bulkhead is the capacity to bear load .That is to say the enhanced bulkhead can bear a bigger force ,because it has a greater thickness ,besides there are some additional component in the bulkhead .The Figure 7.5 shows the strengthen bulkhead where landing gear is fixed .

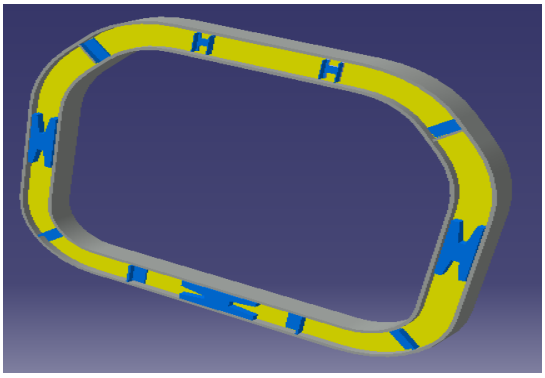

Figure 7.5 Strengthen Bulkhead

(2) The strength checking for bulkhead

Now we simplify the enhanced bulkhead to a circular model, its section is a I-beam ,there are two concentrated forces by cause of landing gear .Figure 7.6 shows the model of enhanced bulkhead .

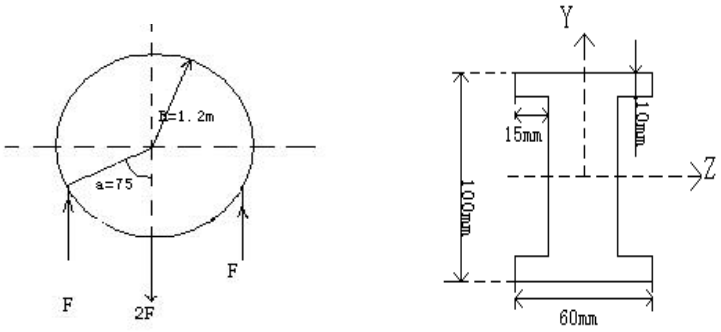

Figure 7.6 Model of Strengthen Bulkhead

The radius of the enhanced bulkhead is about 1.2 meter ,the force caused by landing gear is F ,and the material is LY12 ,its density is 2.8g/cm^3,its allowable stress is 410Mpa .this is a second statically indeterminate structure , Power Law was used to solve this problem.

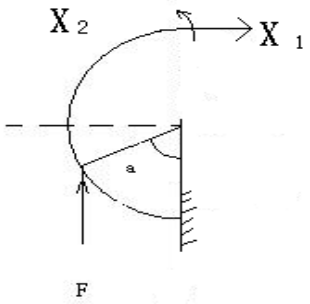

Figure 7.7 Force Analysis

The bending moment is $M_p = FR(\sin\alpha - \sin\varphi)$ $(0 \le \varphi \le \alpha)$, $M_p = 0$ $(\alpha \le \varphi \le \pi)$. Now we use unit power law to calculate relative displacement, in the equation below, M_1 is a supposed unit force, M_2 is a supposed unit torque.

$$\delta_{11} = \frac{1}{EI} R\int_0^{\pi} M_1^2 d\varphi = \frac{9}{2}\pi\frac{R^3}{EI},\quad \delta_{12} = \delta_{21} = \frac{1}{EI} R\int_0^{\pi} M_1 M_2 d\varphi = -2\pi\frac{R^2}{EI},\quad \delta_{22} = \frac{1}{EI} R\int_0^{\pi} M_2^2 d\varphi = \frac{\pi R}{EI}$$

$$\Delta_{1p} = \frac{1}{EI} R\int_0^{\alpha} M_1 M_p d\varphi = \frac{FR^3}{EI}(2\alpha\sin\alpha + 2\cos\alpha - \frac{1}{2}\sin^2\alpha - 2)$$

$$\Delta_{2P} = \frac{1}{EI} R\int_0^{\alpha} M_2 M_p d\varphi = -\frac{FR^2}{EI}(\alpha\sin\alpha + \cos\alpha - 1)$$

By $\begin{cases}\delta_{11}X_1 + \delta_{12}X_2 + \Delta_{1p} = 0\\ \delta_{21}X_1 + \delta_{22}X_2 + \Delta_{2P} = 0\end{cases}$ to get $X_1 = F\dfrac{\sin^2\alpha}{\pi}$, $X_2 = \dfrac{FR}{\pi}\left(\alpha\sin\alpha + \cos\alpha + 2\sin^2\alpha - 1\right)$, then $M = M_p + M_1X_1 + M_2X_2$.

The torque is $M = FR(1 + \pi\sin\alpha - \alpha\sin\alpha - \cos\alpha - \pi\sin\varphi - \sin^2\alpha\cos\varphi)/\pi$ $(0 \le \varphi \le \alpha)$, then $M_{\max} = -0.765FR/\pi$; $M = FR(1 - \alpha\sin\alpha - \cos\alpha - \sin^2\alpha\cos\varphi)/\pi$ $(\alpha \le \varphi \le \pi)$, then $M_{\max} = 0.32FR/\pi$.

Through simple comparison, the biggest torque is $M_{\max} = -0.765FR/\pi$, the negative symbol represent the direction of torque. The biggest stress of enhanced bulkhead is $\sigma_{\max} = M_{\max}y/I_z$. The biggest force F is 3930kg, so we can get the biggest torque is $M_{\max} = 11259.8N$. The inertia moment of section is $I_z = \int y^2 dA = 2\left(\int_0^{0.04} 0.03\times y^2 dy + \int_{0.04}^{0.05} 0.06\times y^2 dy\right) = 3.72\times10^{-6} m^4$, $y = 0.05m$, then $\sigma_{\max} = 156.4Mpa < [\sigma] = 410Mpa$ which meets the strength requirement.

Chapter 8 Flight Performance

Calculation of flight performance are as follows: (1) vertical flight performance calculations including hover ceiling, ground effect hover ceiling, vertical rise rate, rise time, hover efficiency; (2) forward flight performance including power required in forward flight, maximum flight speed, transition speed, tilt climb rate, voyage, cruise duration; (3) the rotation flight performance including minimum rate of glide, minimum angle of glide.

8.1 Vertical Flight Performance

(1) The Process of Calculation

(a) Power required in hover

Compute pull coefficient : $C_T = K_\perp C_G / \left[\frac{1}{2} \rho (\Omega R)^2 \pi R^2 \right]$;Compute lift coefficient of the blade profile: C_{y7} ; Compute profile coefficient C_{x7} according to C_{y7} ; Compute profile power coefficient $m_{kx} = \frac{1}{4} \sigma k_{p0} C_{x7}$; Compute non-dimensional induced velocity in hover: $v_{10} = \frac{1}{2} \sqrt{\frac{C_T}{\kappa}}$; Compute induced power coefficient: $m_{ki} = J_0 v_{10} C_T$; Compute power required coefficient in hover: $m_k = m_{kx} + m_{ki}$; Compute rotor power required in hover: $N_{xy} = m_k \frac{1}{2} \rho (\Omega R)^3 \pi R^2$.

(b) Vertical climb speed

Select the flight altitude, *H*=0~3000*m*, Every other 10 meters for a calculation point; According to the given weight of the helicopter, compute the N_{xy},total power required of the helicopter in hover at every altitude point. Compute the remaining power: $\Delta N = N_{ky} - N_{xy}$; Compute vertical climb speed of the first approximation: $(V_\perp)_1 = \kappa \Delta N / G$; Take into account the induced power of vertical climb is less than the induced power in hover ,the more accurate vertical climb speed should be lager than the first approximation, the second approximation value is : $(V_\perp)_2 = 1.8(V_\perp)_1$; Make the curve of $H - V_\perp$ at every altitude point ,we can get any vertical climb speed $V_\perp$ at any altitude point.

(c) Hover ceiling without ground effect

According to the $H - V_\perp$ curve, to find the altitude point of the corresponding $V_\perp$ =0.5m/s, the altitude is the hover out of ground effect ceiling. Figure 8.1 shows the hover ceiling without ground effect.

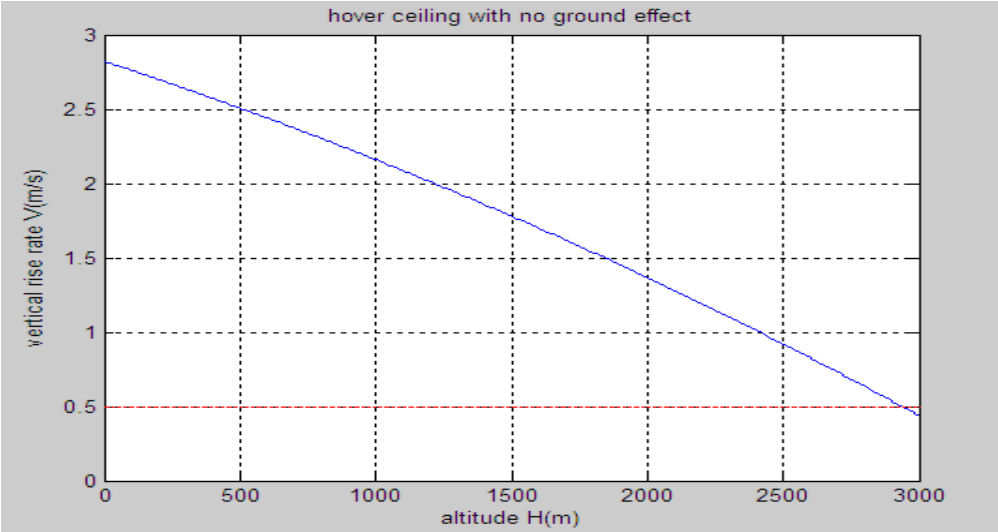

Figure 8.1 Hover Ceiling without Ground Effect

(d) Hover ceiling with ground effect

Repeat the calculation process of calculation of hover out of ground effect ceiling ,rotor power required switch to $N_{xy} = N_{kx} + K_h N_{ki}$,at last make the curve of $H - V_{\perp}$ in ground effect, and find the altitude point of the corresponding $V_{\perp}$ =0.5m/s,the altitude is the hover in ground effect ceiling. The empirical formula of K_h is $1/\left[1+0.038(\frac{2R}{h})^2\right]$, and the so-called hover in ground effect ceiling is the max height to the ground when helicopter wheels from the ground 3 meters high. Figure 8.2 shows the hover ceiling with ground effect.

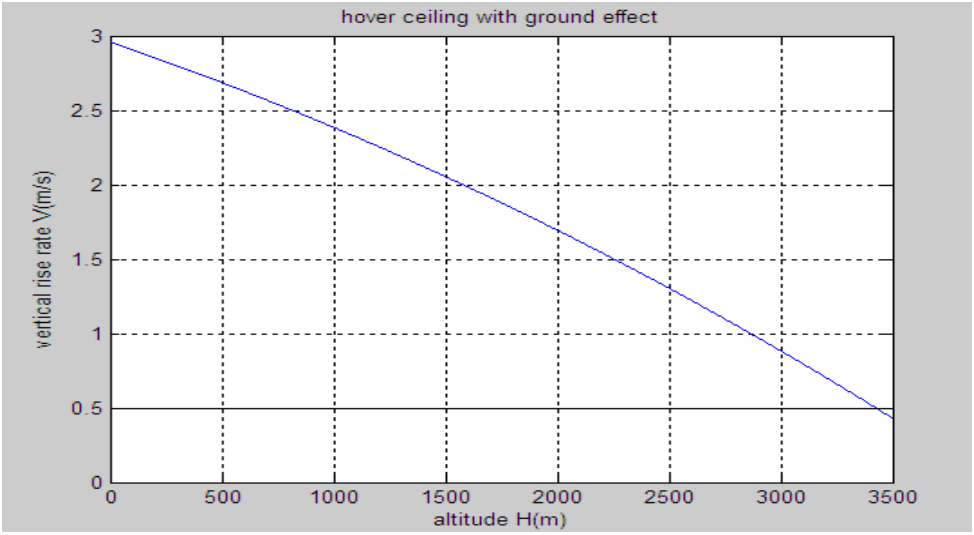

Figure 8.2 Hover Ceiling with Ground Effect

(e) Rise time

Select the altitude , the corresponding value of 0 to $V_{\perp} \approx 0$, Change every other 10 meters; The corresponding value of $V_{\perp}$ found in $H - V_{\perp}$ curve figure as the average of the area; Compute

the rise time of every height $(\Delta t)=\frac{\Delta H}{V_{\perp}}$;Compute the sum of every Δt at the front of any altitude, it is the time that the helicopter need when it climbs to this altitude. According to the time t and making the curve of $H-t$ as shown in Figure 8.3, the time up to any height from the figure can be got.

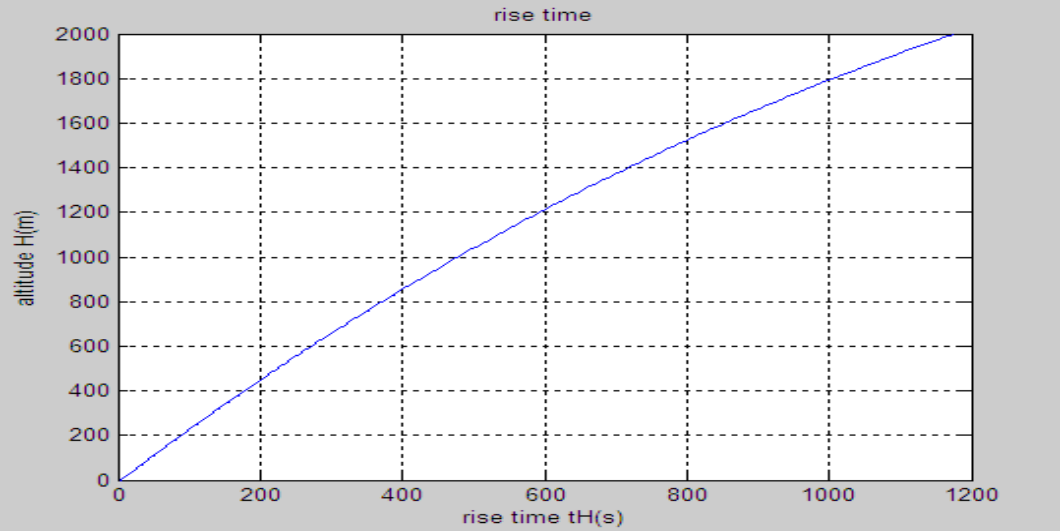

Figure 8.3 Rise Time

(f) Hover efficiency

The hover efficiency is $\eta_0=\frac{TV_{10}}{P_{sj}}$. Taking the coefficient form, $\eta_0=\frac{C_T v_{10}}{m_k}=\frac{1}{2}\frac{C_T^{3/2}}{m_k}$. According to C_T and m_k, the hover efficiency η_0 can be got.

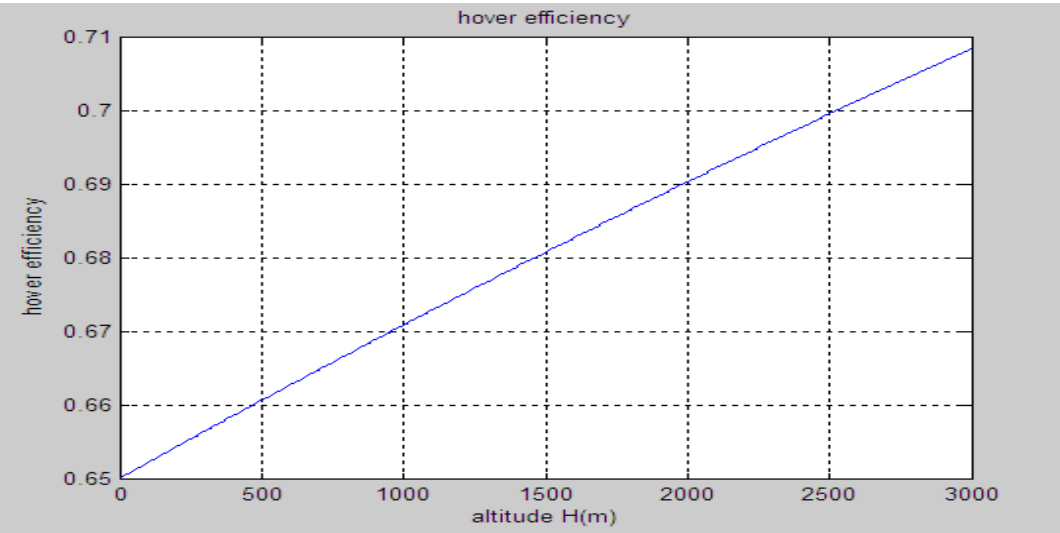

Figure 8.4 Hover Efficiency

(2) Analysis

The vertical flight performance is listed in Table 8.1. It can be seen from Table 8.1 that the

vertical flight performance is better than SA365N, mainly due to the following two reasons: (1) the altitude characteristics of solid rocket jet is better, the output power of solid rocket jet does not change with height; (2) solid rocket jet was installed in the blade tip, gearbox has been omitted, tail rotor has been omitted, so that the efficiency of power transmission has been strengthened. For these two reasons, the vertical flight performance has been upgraded.

Table 8.1 Vertical Flight Performance

Description	unit	Non-conventional	SA365N
hover ceiling	m	2936	1850
ground effect hover ceiling	m	3429	2050
vertical rise rate	m/s	2.69	3.8
rise time(500m)	s	1040	——
hover efficiency		0.66	——

8.2 Forward Flight Performance

(1) The process of calculation

(a) Transition speed

Calculated lift generated by the small wing $L_1 = a_{\infty 1}\alpha_1 \frac{1}{2}\rho V^2 b_1 l$; Calculate lift generated by the rotor $L_2 = G - L_1$; Calculate the angle of attack of rotor $\alpha_2 = L_2 / \left[\frac{1}{2}\rho(\frac{\sqrt{2}}{2}V)^2 bR\right]$; Make a curve about $V \sim \alpha_2$, find the speed corresponds to the allowed angle of attack, that is the transition speed as shown in Figure 8.5.

Figure 8.5 Transition Speed

(b) Maximum flight speed

Calculate the lift generated by the small wing L_1; Calculate the resistance generated by the small wing $D_1 = C_{x1}\frac{1}{2}\rho V^2 b_1 l$; Calculate the lift generated by the rotor $L_2 = G - L_1$; Calculate the rotor airfoil angle of attack α_2; Calculate the rotor airfoil drag coefficient C_x; Calculate the resistance generated by the rotor D_2, divided into two parts: (1) the speed before the transition speed $D_2 = 0$; (2) the speed after the transition speed $D_2 = C_x\frac{1}{2}\rho(\frac{\sqrt{2}}{2}V)^2\frac{\sqrt{2}}{2}bR$; Calculate body resistance; Calculated resistance of the helicopters $D = D_1 + D_2 + D_3$; Calculate the power required $N_{xy} = DV$; Make a curve about $V \sim N_{xy}$ as shown in Figure 8.6, find the speed corresponds to $N_{ky\max}$, that is $V_{\max}$.

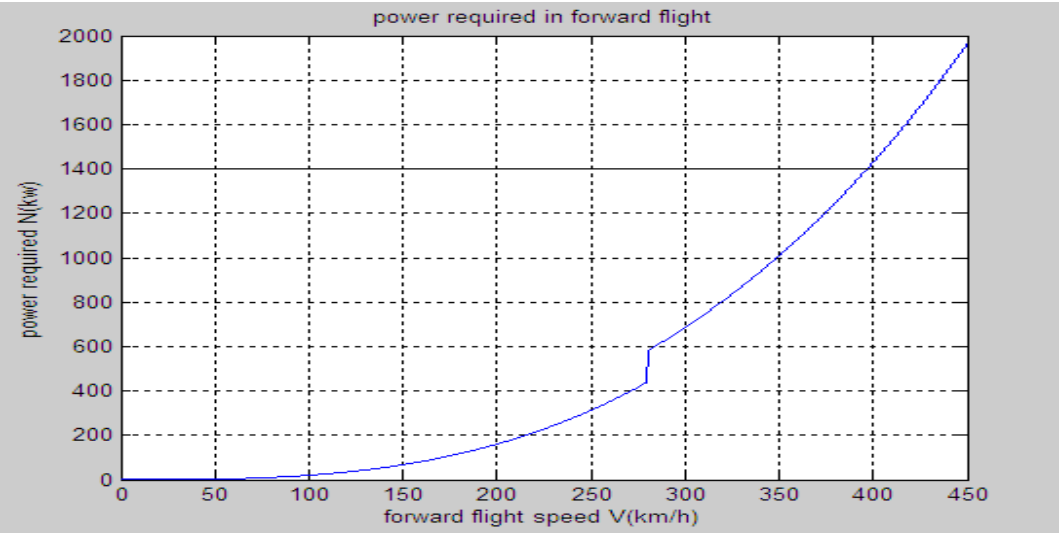

Figure 8.6 Required Power in Forward Flight

(c) Voyage and cruise duration

Calculating voyage $L = \int \frac{dG_{ry}}{q_{KM}} = \frac{\xi G_{ry}}{C_e(N_{xy}/V_0)}$, the voyage vs forward speed is shown in Figure 8.7. Calculating cruise duration $t = \int \frac{dG_{ry}}{q_h} = \frac{\xi G_{ry}}{CeN_{xy}}$, the cruse duration is shown in Figure 8.8.

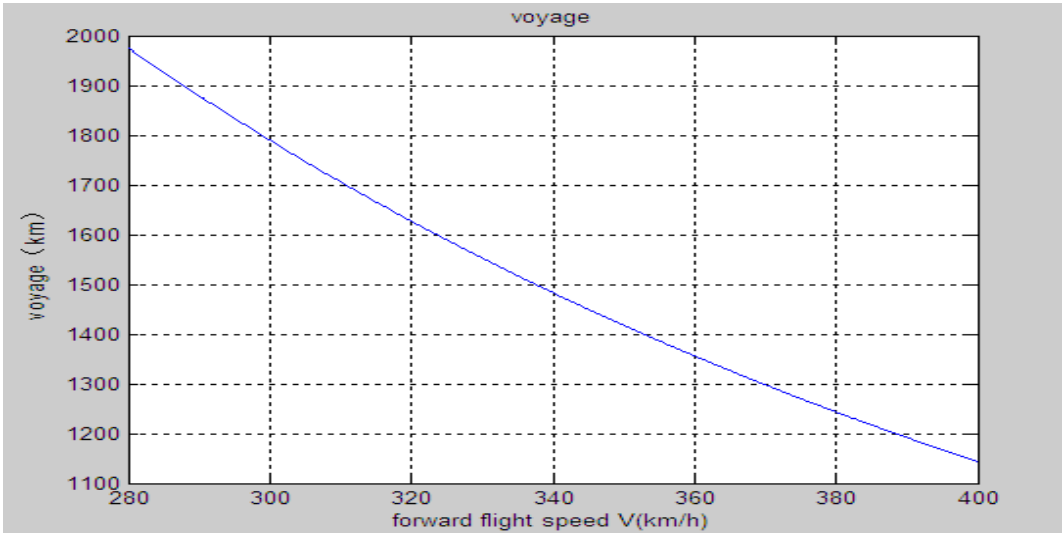

Figure 8.7 Voyage

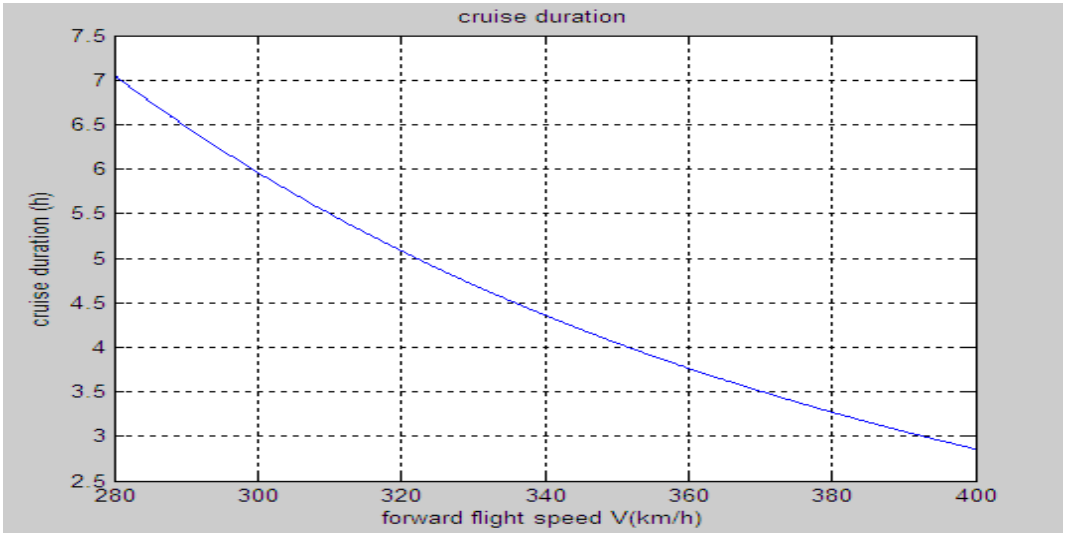

Figure 8.8 Cruise Duration

(d) Tilt climb rate in helicopter flight mode

Calculate $C_T = \dfrac{K_\perp C_G}{\frac{1}{2}\rho(\Omega R)^2 \pi R^2}$; Calculate the blade lift coefficient profile characteristics C_{y7}; Calculate the type resistance coefficient C_{x7}; Calculate the power-type resistance coefficient $m_{kx} = \dfrac{1}{4} C_{x7} \sigma K_{p0}(1+5\mu^2)$; Calculate the induced velocity of hover $v_{10} = \dfrac{1}{2}\sqrt{\dfrac{C_T}{\kappa}}$; Calculate the induced of forward flight speed $v_{dx} = \sqrt{\dfrac{-\mu^2 + \sqrt{\mu^4 + v_{10}^4}}{2}}$; Calculate induced power coefficient

$m_{ki} = C_T v_{dx} J_0 (1+3\mu^2)$; Calculate power required coefficient in forward flight $m_k = m_{kx} + m_{ki}$; Calculate power required in forward flight $N_{xy} = m_k \frac{1}{2} \rho (\Omega R)^3 \pi R^2$; Calculate the tilt climb rate $V_y = k_{ps} \frac{N_{ky} - N_{xy}}{G}$; Make a curve about $V \sim V_y$ as shown in Figure 8.9.

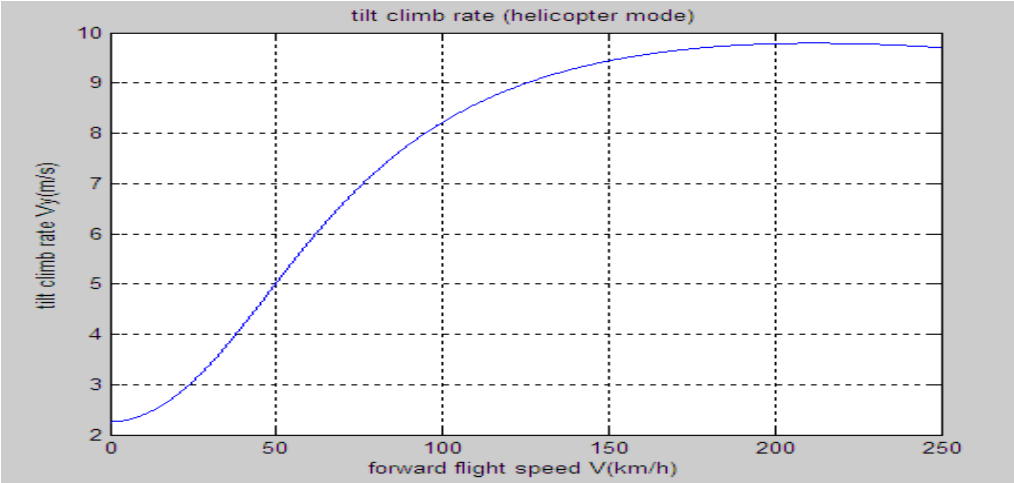

Figure 8.9 Tilt Climb Rate in Helicopter Flight Mode

(e) Tilt climb rate in airplane flight mode

Calculate the power required N_{xy}; Calculate the tilt climb rate $V_y = \frac{\Delta N}{G}$; Make a curve about $V \sim V_y$ as shown in Figure 8.10.

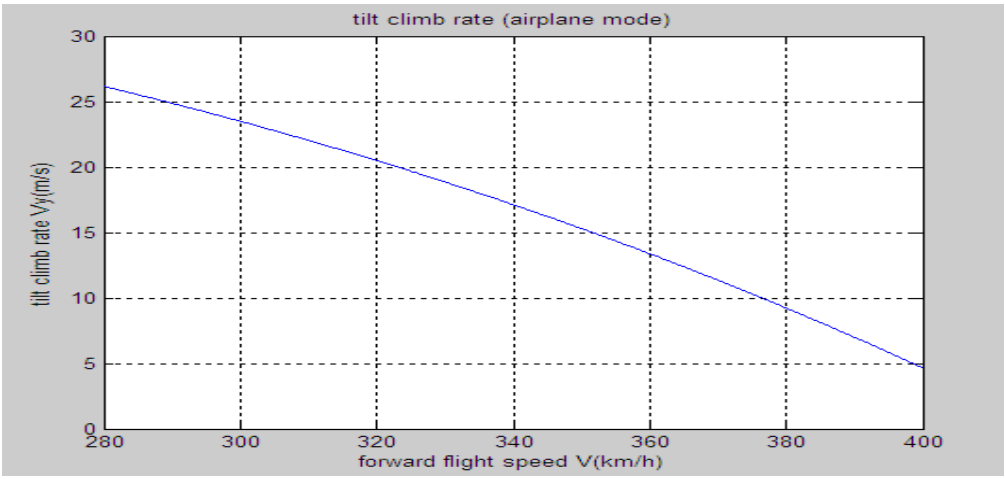

Figure 8.10 Tilt Climb Rate in Airplane Flight Mode

(2) Analysis

The forward flight performance is listed in Table 8.2. It can be seen from Table 8.2 that the maximum flight speed has been upgraded comparing with SA365N, mainly due to changes in the

overall program, the maximum flight speed of a helicopter was major restricted by shock, stall and the dumping of propeller disk. Through configuration changes, we designed the helicopter without such problems, the maximum flight speed limit by the power of engine, which makes it a great speed improvement compared to SA365N. Of course, the maximum flight speed may also be restricted by the impact of structural strength, the paper did not take.

Table 8.2 Forward Flight Performance

Description	Unit	New Helicopter	SA365N
Maximum Flight Speed	km/h	396	306
Transition Speed	km/h	280	——
Tilt Climb Rate(Helicopter Mode)	m/s	9.8	7.7
Tilt Climb Rate(Airplane Mode)	m/s	26	——
Cruise Duration	h	4.05	4.67
Voyage	km	1417.5	882

8.3 Rotation Flight Performance

Calculate rotor power required coefficient of forward flight $m_k = m_{kx} + m_{ki} + m_{kf}$; Calculate rotor power required of forward flight $N_{xy} = m_k \frac{1}{2}\rho(\Omega R)^3 \pi R^2$; Calculate the decline speed $V_y = 1.05\frac{N_{xy}}{G}$; Make a curve about $V \sim V_y$ as shown in Figure 8.11. The minimum rate of glide is 12.2 m/s and the minimum angle of glide is 14.7 degree.

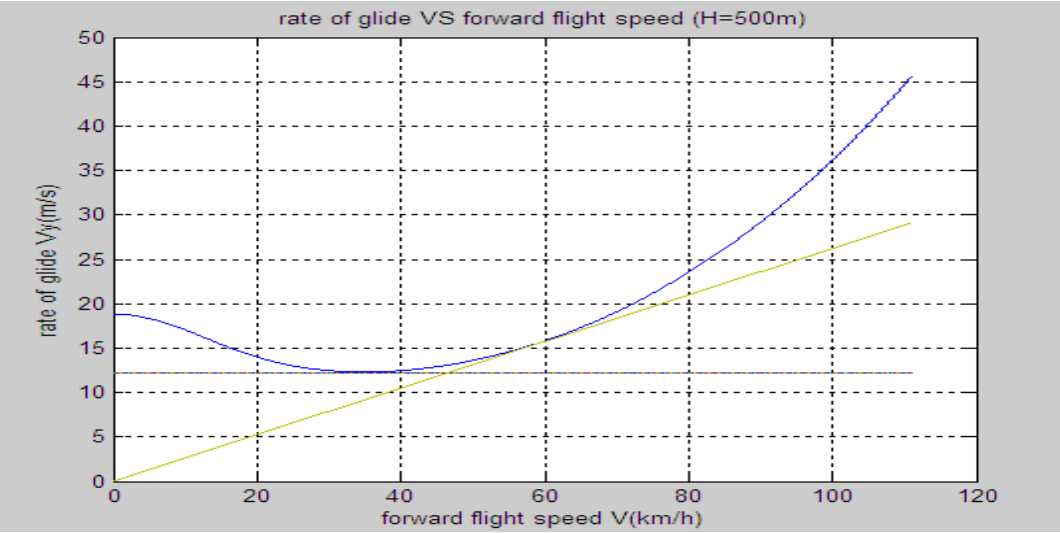

Figure 8.11 Rate of Glide

Acknowledgments

The valuable suggestions for the competition proposal from Prof. Chee Tung of National Aeronautics and Space Administration and Prof. Edward Smith of PennState University are gratefully acknowledged.

The support for the design work from the Lab of Rotor Aeromechanics at Nanjing University of Aeronautics and Astronautics is gratefully acknowledged.

References

[1] Shicun Wang. Helicopter Aerodynamics.Beijing: Nanjing University of Aeronautics and Astronautics Press, 1985.

[2] Xianping Ni. Helicopter Manual.Beijing:Aviation Industry Press,2003.

[3] Chenglin Zhang, Xiaogu Zhang, Shilong Guo. The Design of Helicopter Parts. Nanjing University of Aeronautics and Astronautics Press 1972.

[4] Zhen Gao, Renliang Chen. Helicopter Flight Dynamics. Beijing: Science Press, 2003.

[5] Zhizhao Sun, Qiuting Xiao, Guiqi Xu. Helicopter Strength. Beijing: Aviation Industry Press, 1990.

[6] Huizu Dan. Mechanics of Materials. Beijing: Higher Education Press, 1999.

[7] Pingjian Chen. Several Issues of Helicopter Rotor Aerodynamic Design. Helicopter Technology, 2006,（3）: 60~64.

[8] Dajing Liu.The Analysis of Several Issues in The Development of Composite Rotor Blades. Helicopter Technology,2002,（3）25~28.

[9] Xihong Ding. Structural Mechanics. Nanjing: Nanjing University of Aeronautics and Astronautics Press, 2008.1

[10] Ouwen Liu.Mechanics of Materials.Fourth Edition,BeiJing: Higher Education Press,2004.1

[11] Aircraft Design Manual.First Edition,BeiJing: Aviation Industry Press,1997.10

[12] Naibing Yang,Yinin Zhang. aircraft structural design of composite materials. First Edition,BeiJing: Aviation Industry Press,2004.9

[13] Meizen Tao.Integrated design of modern aircraft structures. First Edition, XiAn: Northwestern Polytechnical University, 2001.3

[14] Zhengneng Li,Yuzhu Zhang,Weiguo Fang. Aircraft structure.

First Edition,BeiJIng: Beijing University of Aeronautics and Astronautics Press,2005.1

[15] Theodorsen. Theory of Propeller, McGraw-Hill Book Company, 1948

[16] Henry.V.B. Summary of Propeller Design Procedures and Data .Volume, AD-774381

[17] Robert T. Taylor,Experimental Investigation of the Effects of Some Shroud Design Varlables on The Static Thrust Characteristics of A Small-Scale Shrouded Propeller Submerged in A Wing, NACA TN 4128, January 1958

[18] Kriebel, A. R.,Predicted and Measured Performance of Two Full-scale Ducted Propellers, NASA CR-578, 1966..

[19] Michael R. Mendenhall and Selden B. Spangler, Theoretical study of ducted fan performance, NASA CR-1494,January 1970.

[20] Andrew B. Connor, Robert J. Tapscott. A flying-qualities study of a small ram-jet helicopter. Washington, NASA, Aprial,1960.

[21] Robert E.Head. Reaction Drive Roters-Lessons Learned. AIAA Aircraft Design Systems Meeting, August 24-26, 1992

[22] Stefan Apostolescu. Turbo Jet Helicopter. United States Patent O ce, Apr. 24, 1956

[23] Marra, John. An expert system eases rotor design. Mechanical Engineering: 1997, Vol. 119 Issue 4, p70.

[24] Yu. S. Stepanov and E. T. Kobyakov.Analytic synthesis of a structurally nonhomogeneous rigid rotor with an inclined disc [J]. Russian Engineering Research: 2007,Volume 27, Number 8,p494-500.

[25] S.J. Setford. Improved operation of a dextran bioreactor-separator through variation of enzyme

activity, viscosity, centrifugal parameters and rotor design. Biotechnology Techniques: 1998,Volume 12, Number 9,p701-705.

[26] Coppinger, Rob. Five-blade bearingless rotor flies. Flight International: 2006, Vol. 169 Issue 5035, p42-42.

[27] Florin Iancu, Janusz Piechna and Norbert Müller.Basic design scheme for wave rotors. Shock Waves : 2008,Volume 18, Number 5,p365-378.

[28] A. Le Pape, P. Beaumier. Numerical optimization of helicopter rotor aerodynamic performance in hover. Applied Aerodynamic Department, ONERA, Châtillon, France, 5 December 2003

[29] Gareth D. Padfield. The Theory and Application of Flying Qualities and Simulation Modelling. Second Edition

[30] R. E. Brown. Comparison of Induced Velocity Models for Helicopter Flight Mechanics. Imperial College of Science

[31] Giorgio Guglieri. Some Aspects of Helicopter Flight Dynamics in Steady Turns. Turin Polytechnic Institute, 10129 Turin, Italyand Roberto Celi University of Maryland, College Park, Maryland 20742.

[32] Dario Fusato, Roberto Celi. Design Sensitivity Analysis for Helicopter Flight Dynamic and Aeromechanic Stability. University of Maryland, College Park, Maryland 20742-3015

[33] K. Hughes, J. Campbell, R. Vignjevic. Application of the finite element method to predict the crashworthy response of a metallic helicopter under floor structure onto water. Crashworthiness, Impacts and Structural Mechanics Group, School of Engineering, Cranfield University, Cranfield, BEDS MK43 0AL, UK. Received 10 June 2006; received in revised form 22 August 2006; accepted 24 March 2007

[34] Chiara Bisagni. Crashworthiness of helicopter subfloor structures. Dipartimento di Ingegneria Aerospaziale, Politecnico di Milano, Via La Masa 34, 20158 Milano, Italy. Received 13 November 2000; received in revised form 9 November 2001; accepted 22 February 2002

[35] M.A. McCarthy, J.F.M. Wiggenraad. Numerical investigation of a crash test of a composite helicopter structure. Department of Mechanical and Aeronautical Engineering, University of Limerick, Limerick, Ireland, National Aerospace Laboratory NLR, Voorsterweg 31, P.O. Box 153, 8300 AD Emmeloord, Netherlands

[36] M.J. Ostrander, J.L. Bergmans, M.E. Thomas, and S.L. Burroughs Pintle motor challenges for tactical missiles. AIAA-2000-3310, July, 2000

[37] J.W Coon, Pintle Pulse Motors—An Alternative Approach, CPIA Publication 340, VOL.IV, May 1981, pp.223—254

[38] Smith-Kent, RandallLoh, Hai-TienChwalowski, Pawel, Analytical contouring of pintle nozzle exit cone using computational fluid dynamics. AIAA-1995-2877 July 10-12,1995

[39] S.G. Rock, S. D. Habchi, and T. J. Marquette. Numerical simulation of controllable propulsion for advanced escape syetems. AIAA-1997-2254, June 1997

[40] Andre Lafond. Numerical simulation of the flowfield inside a hot gas valve. AIAA-1999-1087 Jan,1999

[41] Yasuhara W. K. Advanced gel propulsion controls for kill vehicles.AIAA-93-2636